Akari, H., Fujita, M., Kao, S., Khan, M.A., Shehu--Xhilaga, M., **Adachi, A.**, and Strebel, K.	High level expression of Human Immunodeficiency Virus type-1 Vif inhibits viral infectivity by modulating proteolytic processing of the Gag precursor at the p2/NC processing site.	J. Biol. Chem.	279	12355-12362	2004
Sugahara, F., Uchiyama, T., Watanabe, H., Shimazu, Y., Kuwayama, M., Fujii, Y., Kiyotani, K., **Adachi, A.**, Kohno, N., Yoshida, T., and Sakaguchi, T.	Paramyxovirus Sendai virus-like particle formation by expression of multiple viral proteins and acceleration of its release by C protein	Virology	325	1-10	2004
Piroozmand, A., Koyama, A.H., Shimada, Y., Fujita, M., Arakawa, T., and **Adachi, A.**	Role of Us3 gene of herpes simplex virus type 1 for resistance to interferon	Int. J. Mol. Med.	14	641-645	2004
高折晃史					
Noguchi, C., Hiraga, N., Mori, N., Tsuge, M., Imamura, M., Takahashi, S., Fujimoto, Y., Ochi, H., Abe, H., Maekawa, T., Yatsuji, H., Shirakawa, K., **Takaori-Kondo, A.**, and Chayama, K.	Dual Effect of APOBEC3G on Hepatitis B Virus.	J. Gen. Virol.			In press
Aierken Abudu, **Takaori-Kondo, A.**, Izumi, T., Shirakawa, K., Kobayashi, M., Sasada, A., Fukunaga, K., and Uchiyama, T.	Murine retrovirus escapes from murine APOBEC3 via 2 distinct novel mechanisms.	Curr. Biol.	16	1565-1570	2006
Takaori-Kondo A.	APOBEC Family Proteins: Novel Antiviral Innate Immunity.	Int. J. Hematol.	83	213-216	2006
Tanaka, Y., Marusawa, H., Seno, H., Matsumoto, Y., Ueda, Y., Kodama, Y., Endo, Y., Yamauchi, J., Matsumoto, T., **Takaori-Kondo, A.**, Ikai, I., and Chiba, T.	Anti-viral protein APOBEC3G is induced by Interferon-α Stimulation in Human Hepatocytes.	Biochem. Biophys. Res. Commun.	341	314-319	2006
Shirakawa, K., **Takaori-Kondo, A.**, Kobayashi, M., Tomonaga, M., Izumi, T., Fukunaga, K., Sasada, A., Aierkin Abudu, Miyauchi, Y., Akari, H., Iwai, K., and Uchiyama, T.	Ubiquitination of APOBEC3 proteins by the Vif-Cullin5-ElonginB-ElongiC complex.	Virology	344	263-266	2006
高折晃史	HIV-1 とユビキチン	蛋白質核酸酵素	51	1433-1436	2006
高折晃史	HIV-1 の対ホスト戦略	感染・炎症・免疫	36	106-111	2006
櫻木淳一					
Ohishi M., T. Shioda, and **J. I. Sakuragi**.	Retro-transduction of virus pseudotyped with glycoprotein of vesicular stomatitis virus.	Virology			In press
Sakuragi, S., **Sakuragi, J. I.**, Morikawa, Y., and Shioa, T.	Development of a rapid and convenient method for the quantification of HIV-1 budding.	Microbes Infect.	8	1875-1881	2006
櫻木淳一	レトロウイルス粒子内ゲノム２量体化機構の解析	蛋白質核酸酵素	50	892-899	2005

櫻木淳一	霊長類レンチウイルス粒子内ゲノム二量体化機構の解析	ウイルス	55	153-160	2005
高橋秀宗					
Maeda, M., Sawa, H., Tobiume, M., Tokunaga, K., Hasegawa, H., Ichinohe, T., Sata, T., Moriyama, M., Hall, W.W., Kurata, K., and **Takahashi, H.**	Tristetraprolin inhibits HIV-1 production by binding to genomic RNA.	Microbes Infect.	8	2647-2656	2006
Hasegawa, H., Sawa, H., Lewis, M.J., Orba, Y., Sheehy, N., Yamamoto, Y., Ichinohe, T., Tsunetsugu-Yokota, Y. Katano, H., **Takahashi, H.**, Matsuda, J., Sata, T., Kurata, T., Nagashima, K., and Hall, W.W.	Thymus-derived leukemia-lymphoma in mice transgenic for the Tax gene of human T-lymphotropic virus type I.	Nat. Med.	12	466-472	2006
Takahashi, H., Maeda, M., Sawa, H., Hasegawa, H., Moriyama, M., Sata, T., Hall, W.W., and Kurata, T.	Dicer and positive charge of proteins decrease the stability of RNA containing the AU-rich element of GM-CSF.	Biochem. Biophys. Res. Commun.	340	807-814	2006
Okada, Y., Suzuki, T., Sunden, Y., Orba, Y., Kose, S., Imamoto, N., **Takahashi, H.**, Tanaka, S., Hall, W.W., Nagashima, K., and Sawa, H.	Dissociation of heterochromatin protein 1 from lamin B receptor induced by human polyomavirus agnoprotein: role in nuclear egress of viral particles.	EMBO Rep.	6	452-457	2005
Harada, T., Tatsumi, M., **Takahashi, H.**, Sata, T., Kurata, T., and Kojima, A.	Specific reactions between purified HIV-1 particles and CD4(+)cell membrane fragments in a cell-free system of virus fusion or entry.	Microbes Infect.	6	421-428	2004
Takahashi, H., Sawa, H., Hasegawa, H., Nagashima, K., Sata, T., and Kurata, T.	Topoisomerase I dissociates human Immunodeficiency virus Type 1 (HIV-1) reverse transcriptase from genomic RNAs.	Biochem. Biophys. Res. Commun.	313	1073-1078	2004
Ueno, T., Tokunaga, K., Sawa, H., Maeda, M., Chiba, J., Kojima, A., Hasegawa, H., Shoya, Y., Sata, T. Kurata, T. and **Takahashi, H.**	Nucleolin and the packaging signal, ϕ promote the budding of human immunodeficiency virus type-1 (HIV-1).	Microbiol. Immunol.	48	111-118	2004
駒野　淳					
Shimizu S, Urano E, Futahashi Y, Miyauchi K, Isogai M, Matsuda Z, Nohtomi K, Onogi T, Takebe Y, Yamamoto N, **Komano J.**	Inhibiting lentiviral replication by HEXIM1, a cellular inhibitor of cdk9/cyclinT complex.	AIDS			In press
Futahashi Y, **Komano J.**, Urano E, Aoki T, Hamatake M, Miyauchi K, Yoshida T, Koyanagi Y, Matsuda Z, Yamamoto N.	Separate elements are required for ligand-dependent and –independent internalization of metastatic potentiator CXCR4.	Cancer Science			In press

Miyauchi, K., **Komano, J.**, Myint, L., Futahashi, Y., Urano, E., Matsuda, Z., Chiba, T., Miura, H., Sugiura, W., and Yamamoto, N.	Rapid propagation of low-fitness drug-resistant mutants of humanimmunodeficiency virus type 1 by a streptococcal metabolite sparsomycin.	Antivir. Chem. Chemother.	17	167-174	2006
Miyauchi, K., Curran, R., Matthews, E., **Komano, J.**, Hoshino, T., Engelman, DM., and Matsuda, Z.	Mutations of conserved glycine residues within the membrane-spanning domain ofhuman immunodeficiency virus type 1 gp41 can inhibit membrane fusion andincorporation of Env onto virions.	Jpn. J. Infect. Dis.	59	77-84	2006
Komano, J., Futahashi, Y., Urano, E., Miyauchi, K., Murakami, T., Matsuda, Z., and Yamamoto, N.	The interaction of HIV-1 with the host factors.	Jpn. J. Infect. Dis.	58	125-130	2005
Miyauchi, K., **Komano, J.**, Yokomaku,, Y., Sugiura, W., Yamamoto, N., and Matsuda, Z.	Role of the specific amino acid sequence of the membrane-spanning domain of human immunodeficiency virus type 1 in membrane fusion.	J. Virol.	79	4720-4729	2005
山本直樹、松田善衛、村上努、**駒野　淳**	AIDS の新たな治療標的を求めて：HIV-1 の宿主因子.	実験医学	23	2068-2073	2005
Komano, J., Miyauchi, K., Matsuda, Z., and Yamamoto, N.	Inhibiting the Arp2/3 complex limits infection of both intracellular maturevaccinia virus and primate lentiviruses.	Mol. Biol. Cell	15	5197-5207	2004
西澤雅子					
Chiba-Mizutani T, Miura H, Matsuda M, Matsuda Z, Yokomaku Y, Miyauchi K, **Nishizawa M**, Yamamoto N, Sugiura W.	New T-Cell-Based Lines with Two Luciferases for Accurately Evaluating Susceptibility to HIV-1 Drugs.	J Clin Microbiol.			In press
Kondo, M., Shima, T., **Nishizawa, M.**, Sudo, K., Iwamuro, S., Okabe, T., Takebe, Y., and Imai, M.	Identification of attenuated variants of HIV-1 circulating recombinant form 01_AE that are associated with slow disease progression due to gross genetic alterations in the nef/long terminal repeat sequences.	J. Infect. Dis.	192	56-61	2005
Yan, H., Mizutani, T.C., Nomura, N., Takakura, T., Kitamura, Y., Miura, H., **Nishizawa, M.**, Tatsumi, M., Yamamoto, N., and Sugiura, W.	A novel small molecular weight compound with a carbazole structure that demonstrates potent human immunodeficiency virus type-1 integrase inhibitory activity.	Antivir. Chem. Chemother.	16	363-373	2005

III. 刊行物別刷り(抜粋)

JOURNAL OF VIROLOGY, Sept. 2005, p. 12045–12057 Vol. 79, No. 18
0022-538X/05/$08.00+0 doi:10.1128/JVI.79.18.12045–12057.2005

Human Immunodeficiency Virus Mutagenesis during Antiviral Therapy: Impact of Drug-Resistant Reverse Transcriptase and Nucleoside and Nonnucleoside Reverse Transcriptase Inhibitors on Human Immunodeficiency Virus Type 1 Mutation Frequencies

Renxiang Chen,[1,4]† Masaru Yokoyama,[5] Hironori Sato,[5] Cavan Reilly,[1,3] and Louis M. Mansky[1,2]*

Institute for Molecular Virology,[1] Departments of Diagnostic and Biological Sciences and Microbiology,[2] and Department of Biostatistics,[3] University of Minnesota, Minneapolis, Minnesota 55455; Biochemistry Graduate Program, Ohio State University, Columbus, Ohio 43210[4]; and Division of Molecular Genetics, National Institute of Infectious Diseases, Tokyo, Japan[5]

Received 21 April 2005/Accepted 21 June 2005

The development of antiviral drug resistance is an important problem in the treatment of human immunodeficiency virus type 1 (HIV-1) infection. Potent antiretroviral therapy is currently used for treatment, and typically consists of at least two reverse transcriptase (RT) inhibitors. We have previously reported that both drugs and drug-resistant RT mutants can increase virus mutation frequencies. To further assess the contributions of nucleoside RT inhibitors (NRTIs), nonnucleoside RT inhibitors (NNRTIs), and drug-resistant RTs to HIV mutagenesis, a new high-throughput assay system was developed. This assay system was designed to specifically detect frameshift mutations in the luciferase gene in a single virus replication cycle. New drug-resistant RTs were identified that significantly altered virus mutation frequencies. Consistent with our previous observations of NRTIs, abacavir, stavudine, and zalcitabine increased HIV-1 mutation frequencies, supporting the general hypothesis that the NRTIs currently used in antiviral drug therapy increase virus mutation frequencies. Interestingly, similar observations were made with NNRTIs. This is the first report to show that NNRTIs can influence virus mutation frequencies. NNRTI combinations, NRTI-NNRTI combinations, and combinations of drug and drug-resistant RTs led to significant changes in the virus mutation frequencies compared to virus replication of drug-resistant virus in the absence of drug or wild-type virus in the presence of drug. This indicates that combinations of RT drugs or drugs and drug-resistant virus created during the evolution of drug resistance can act together to increase HIV-1 mutation frequencies, which would have important implications for drug therapy regimens. Finally, the influence of drug-resistant RT mutants from CRF01_AE viruses on HIV-1 mutation frequencies was analyzed and it was found that only a highly drug resistant RT led to altered virus mutation frequencies. The results further suggest that high-level drug-resistant RT can significantly influence virus mutation frequencies. A structural model that explains the mutation frequency data is discussed.

Potent antiretroviral therapy of human immunodeficiency virus type 1 (HIV-1) infection with antiretroviral drugs consists of nucleoside RT inhibitors (NRTIs), nonnucleoside RT inhibitors (NNRTIs), and protease inhibitors. Antiretroviral drugs have been previously shown to influence HIV-1 mutation frequencies and the HIV-1 mutation rate. The first study of the impact of drugs on HIV-1 mutation frequencies was investigating how the NRTIs 3′-azido-3′-deoxythymidine (zidovudine) and (−)2′,3′-dideoxy-3′-thiacytidine (lamivudine) influence HIV-1 mutation frequencies (24). These analyses used the *lacZ*α peptide gene as a mutation target that has been used in previous mutation rate studies of HIV-1.

Zidovudine increased the HIV-1 mutation frequency by 7.6-fold in a single round of replication, while lamivudine led to a 3.4-fold increase in virus mutation frequency. How NRTIs increase HIV-1 mutagenesis is presently not known, but the NRTIs currently used in therapy may have a similar mechanism to influence HIV-1 mutation frequencies. This is supported by the observation that HIV-1 mutation frequencies increased in an additive manner during virus replication in the presence of two NRTIs (i.e., zidovudine and lamivudine, zidovudine and dideoxyinosine, and lamivudine and dideoxyinosine) (23).

Zidovudine-resistant RT was also found to increase the virus mutation frequency by 4.3-fold, but the replication of lamivudine-resistant HIV-1 had no significant influence on the mutation frequency (24). Furthermore, it was observed that only high-level zidovudine-resistant RT mutants could influence the in vivo mutation frequency, such as those containing mutations M41L/T215Y and M41L/D67N/K70R/T215Y. These observations suggested that when virus replication occurs in the presence of suboptimal concentrations of drug, drug-resistant virus

* Corresponding author. Mailing address: Institute for Molecular Virology, 18-242 Moos Tower, 515 Delaware St. SE, Minneapolis, MN 55455. Phone: (612) 626-5525. Fax: (612) 626-5515. E-mail: mansky@umn.edu.

† Present address: Department of Microbiology and Immunology, Georgetown University, Washington, D.C.

is selected and that replication of drug-resistant virus in the presence of drug could further increase the virus mutation rate.

To test this hypothesis, the combined effects of drug and drug-resistant virus were investigated (26). It was found that replication of zidovudine-resistant virus in the presence of zidovudine led to a multiplicative 24-fold increase in the virus mutation frequency compared to that observed with wild-type virus in the absence of drug. In addition, it was found that replication of a zidovudine/lamivudine dual-resistant virus in the presence of both zidovudine and lamivudine also led to a multiplicative 22.5-fold increase in the virus mutation frequency. These results indicated that when drug failure occurs due to the evolution of drug resistance, replication of the drug-resistant virus in the presence of drug could significantly increase HIV-1 mutagenesis.

Previous in vitro studies using purified HIV-1 RT showed that single base substitutions and single base frameshift mutations were predominant mutations in the HIV-1 mutational spectrum and were nonrandomly distributed (3). Most of these mutations were found at mutation hot spots, typically homopolymeric runs. It was observed that many single base substitutions occurred at either the 5′ end or the 3′ end of homopolymeric runs, indicating many single base substitutions, as well as frameshift mutations, are initiated by template-primer slippage (3, 4). Consistent with these observations, the homopolymeric runs were found to be hot spots for spleen necrosis virus RT to initiate frameshift mutations (most common mutations were +1 and −1) in a single round of viral replication (7). The mutation rate for runs of T's was the highest compared to rates for runs of A's, C's, and G's.

Moreover, the analysis of the HIV-1 mutation rate in a single round of replication also demonstrated that both base substitutions and frameshift mutations were common mutations during HIV-1 reverse transcription; the most common frameshift mutations were +1 mutations at a run of T's (28). Further study of mutations in HIV-1 proviruses following treatment with antiretroviral drugs showed that the mutation spectra of HIV-1 after drug treatment was comparable to the spectrum of mutants observed in the absence of drugs, indicating that the mechanisms by which mutations occurred were similar but that the rate had increased (24).

In order to extend our current knowledge of how antiretroviral drugs and drug-resistant RTs influence HIV-1 mutation frequencies, a new high-throughput assay system using the *luc* gene as a mutational target was developed to measure HIV-1 mutation frequencies based on previous observations (3, 4, 7, 24, 28). Using this new assay system several issues were addressed. First, specific mutations in HIV-1 RT that conferred resistance to antiretroviral drugs were tested to determine if they could influence the rate of HIV-1 mutation. Second, the hypothesis that the NRTIs currently used in drug therapy could increase HIV-1 mutation frequencies was tested. Third, it was tested whether NNRTIs could influence HIV-1 mutation frequencies. Fourth, the combined effects of drugs and of drugs and drug-resistant RTs on virus mutation frequencies were found to alter HIV-1 mutation frequencies. Finally, it was observed that high-level drug-resistant RT mutants from CRF01_AE viruses could significantly influence HIV-1 mutation frequencies.

MATERIALS AND METHODS

Retroviral vectors and expression plasmids. HIV-SVLuc8T was developed to measure the reversion mutation rate of HIV-1 using a mutated *luc* gene as the reporter. This vector was designed to specifically detect frameshift mutations in the luciferase gene in a single virus replication cycle. Eight T residues were inserted after the *luc* gene start codon by two-step PCR mutagenesis using the pGL3 control vector as the template. This insertion causes the complete loss of luciferase activity due to the loss of the open reading frame. A 1.5-kb deletion (from the SalI to NheI sites) within the open reading frame of the *env* gene was made in the HIV vector KP97 (graciously provided by Michael Emerman, Fred Hutchinson Cancer Research Center, Seattle, Wash.), which is an HIV vector derivative of pBRU2 with a 3.1-kb deletion (SphI to BglI) of the *gag* and *pol* genes. This *env* deletion was replaced with a 1.9-kb XhoI to XbaI fragment from pGL3, which contains the simian virus 40 promoter and the mutated *luc* gene (Fig. 1A).

The HIV-1 *gag-pol* expression plasmid used was pSVgagpol-rre-MPMV, which has been described previously (27). This expression vector contains the simian virus 40 promoter driving expression of the HIV-1 *gag-pol* genes. The vector used for expression of vesicular stomatitis virus glycoprotein envelope, pHCMV-G, was obtained J. Burns (University of California at San Diego, San Diego, CA). To be packaged into virus particles, HIV-SVLuc8T was complemented in *trans* with the HIV-1 *gag-pol* expression plasmid and pseudotyped with the vesicular stomatitis virus G envelope expression plasmid.

The HIV-1 RT mutants (subtype B) analyzed in these experiments were constructed by introducing mutations coding for RT amino acid substitutions into pSVgagpol-rre-MPMV by site-directed mutagenesis (Quick Change, Stratagene, La Jolla, CA). The helper vectors containing HIV-1 CRF01_AE RT variants were created by deletion of full-length CRF01_AE clones (p93JP-NH1 and its variants). The mutant RT genes confer different levels of NRTI resistance in the genetic backbone of 93JP-NH1 virus (38). A 2.4-kb deletion was made in each of the full-length CRF01_AE clones between the two AvrII sites. This deletion removed the *vpr*, *tat*, and *env* genes of CRF01_AE, so that these gene products will be supplied by the other plasmid constructs.

Cell culture and antiretroviral drugs. 293T cells were maintained in Dulbecco's modified Eagle's medium (GIBCO BRL, Gaithersburg, MD), supplemented with 10% of fetal clone III serum (HyClone, Logan, UT). MAGI cells were maintained in Dulbecco's modified Eagle's medium supplemented with 10% of fetal clone III serum, G418 (0.2 mg/ml), and hygromycin (0.1 mg/ml). Virus-infected cells were scored by staining MAGI cells with 5-bromo-4-chloro-3-indolyl-β-D-galactopyranoside (X-Gal).

Antiretroviral drugs were obtained from the National Institutes of Health AIDS Research Reagents Program (Bethesda, MD) except for lamivudine, which was purchased from Sigma (St. Louis, MO).

Transfections and infections. The experimental protocol developed to obtain a single round of HIV-1 vector replication is shown in Fig. 1B, and described in detail elsewhere (28). Briefly, HIV-SVLuc8T (9.5 μg) was cotransfected with pSVgagpol-rre-MPMV (9.5 μg) and vesicular stomatitis virus G (1 μg) into 293T cells in a 100-mm petri dish using the calcium phosphate precipitation method. Viruses were harvested 48 h posttransfection and concentrated using a Centricon Plus-20 filter (Millipore, Billerica, MA). For infections, concentrated virus was mixed with Polybrene (8 μg/ml) (Sigma, St. Louis, MO) and the virus-Polybrene mixture was used to infect two sets of fresh MAGI target cells (2.5×10^5 cells per dish). After 24 h, cells were washed once with phosphate-buffered saline (GIBCO BRL), and fresh medium was added. The cells were then incubated at 37C for an additional 48 h. Supernatants were removed, and one set of cells was used to perform the MAGI assay to determine virus titer (17). The other set of cells was lysed and used for the luciferase assay to detect the restored luciferase activity (Fig. 1B). Cell numbers at the time of these assays were typically 5×10^5 to 10×10^5 cells.

Reversion mutation detection. Mutations that restored luciferase activity were determined in MAGI cells, which were treated or not with antiretroviral drugs. Drug treatments were typically done by maintaining MAGI target cells in medium supplemented with drug at the 50% inhibitory concentration (IC_{50}) from 2 h prior to infection and until 24 h after infection. Seventy-two hours postinfection, infected MAGI cells were counted using the trypan blue dye exclusion method, harvested, and lysed in 1× luciferase assay lysis buffer (25 mM Tris-phosphate [pH 7.8], 2 mM dithiothreitol, 2 mM 1,2-diaminocyclohexane-*N*,*N*,*N*′,*N*′-tetracetic acid, 10% glycerol, 1% Triton X-100). Luciferase activity was quantified using the Promega Luciferase Assay System (Promega, Madison, WI). Mutation frequencies were calculated based on luciferase activity reading, viral titer, and cell numbers. The relative mutation frequency of wild-type viruses that were not treated with drug was defined as 1. The equation used to calculate the relative mutation frequencies (RMF) is RMF = {[(number of cells with no

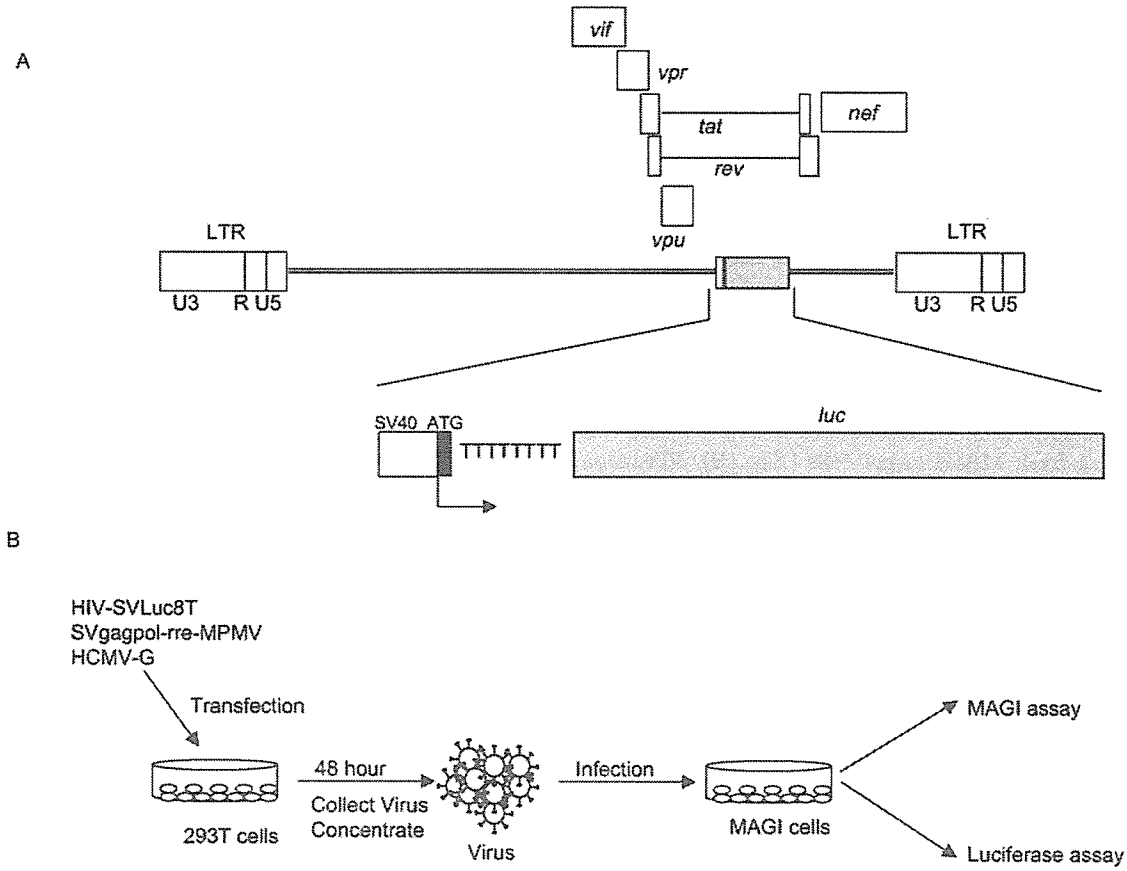

FIG. 1. Assay system used for analysis of virus mutation frequencies. (A) Schematic representation of the HIV-1 vector used to analyze HIV-1 mutation frequencies. The proviral DNA form of the vector is shown. The large rectangular boxes are long terminal repeats, which include U3, R, and U5. The simian virus 40 promoter (SV40), *luc* gene, and *luc* gene start codon are indicated. (B) Single round of replication assay for mutation frequencies. Virus-producing cells were transfected with HIV-1 reporter vector and helper plasmids, and the viruses produced were concentrated and used to infect fresh MAGI cells. The MAGI assay and luciferase assay were used to determine the reverse mutation frequencies.

drug treatment/number of cells with drug treatment) × luciferase reading of drug-treated cells]/luciferase reading of cells with no drug treatment} × (viral titer of virus with no drug treatment/viral titer of drug-treated virus).

Determination of 50% inhibitory concentrations. The MAGI assay was used to determine the IC_{50} value for each drug. Briefly, 2.5×10^5 fresh MAGI target cells were treated with antiretroviral drug at different concentrations 2 h prior to infection and continued until 24 h postinfection. Virus-Polybrene mixture was diluted to 1:1,000 and used to infect MAGI target cells. Seventy-two hours postinfection, infected MAGI cells were stained with X-Gal and positive blue cells were counted to determine virus titer at each concentration. The virus titer was plotted as a function of the drug concentration used, generating linear curves for all the drugs. IC_{50} values for each drug were calculated based on the linear plots (Fig. 2).

Analysis of mutation spectra. Cellular DNA was prepared from 10^5 cells infected by wild-type HIV-1 in the absence of drug. Following infection, the infected MAGI cells were washed once with phosphate-buffered saline, trypsinized and lysed in 500 μl of PCR lysis buffer (50 mM KCl, 10 mM Tris, pH 8.3, 1.8 mM $MgCl_2$, 0.45% IGEPAL CA-630, 0.45% Tween 20). The cell lysate was treated with 3 μl of proteinase K (20 mg/ml) (Roche, Indianapolis, IN) at 50°C for 1 h. The 5′ end of the *luc* gene was amplified from cell lysate using nested PCR. The PCR products were then cloned into pCR2.1 TA cloning vector (Invitrogen, Calsbad, CA). The plasmid DNAs were isolated and sequenced.

Statistical analysis. To investigate the effects of antiretroviral drugs and RT variants on mutation frequency, we fit a linear model to the normalized logarithms of the fold changes relative to the wild type. Normalization was conducted as described above. The model pooled data from all experiments and replicates to estimate effects for each drug and RT variant in addition to all estimable interactions. The model supposes that assay variability is constant across all conditions and replicates, an assumption that is consistent with the data. The model has a term for all drugs and RT variants in addition to interactions. Standard diagnostic techniques failed to reveal any major shortcomings of the model. Ninety-five percent confidence intervals for all fold changes were constructed by sampling parameters from their joint sampling distribution and then transforming the parameters (i.e., exponentiating) to obtain samples from the joint sampling distribution of the fold changes. We summarize the results with the upper and lower endpoints of these intervals in addition to the estimate of the fold change.

Structural analysis. To investigate the initial binding sites of deoxynucleoside triphosphates and NRTIs with HIV-1 RT, we used the crystal structure of the RT-template-primer complex at a resolution of 3.1Å from the Protein Data Bank (PDB code 1N5Y) (37) as a template for substrate docking simulations. This structure represents an open configuration at the posttranslocation stage during the catalytic cycle of RT, which theoretically is competent for binding of the incoming-substrate. The template was docking with deoxynucleoside triphosphate and deoxynucleoside triphosphate analogs by using the automated ligand docking program AS_Dock (Ryoka Systems Inc., Chiba, Japan) operated in the Molecular Operating Environment. The precision of docking results with the AS_Dock is generally equivalent to the experimental error (i.e., a few angstroms). In fact, a result of dTTP docking with the AS_Dock at the catalytic site in an RT closed configuration had a root-mean-square deviation of ~1.6 Å compared to that determined by x-ray crystallography (1RTD) (11), which was the range within the resolution of the crystal structure.

RESULTS

Development of a new high-throughput assay system to measure HIV-1 mutation frequencies. Previous studies of HIV-1 mutation frequencies used the *lacZα* gene as a reporter

gene (28). However, using this system is laborious and time-consuming. In order to more rapidly assess the ability of drugs and/or drug-resistant RTs to influence HIV-1 mutation frequencies, a new high-throughput assay system was developed. This system was designed to be a reversion assay that would specifically detect frameshift mutations in the luciferase reporter gene in a single round of replication (3, 4, 7, 24, 28) (Fig. 1).

The HIV-1 vector developed contained a mutated *luc* gene, which was inserted into the *env* gene. Specifically, eight T residues were inserted after the start codon of the *luc* gene (Fig. 1A). To be packaged into virus particles, the vector was complemented in *trans* with an HIV-1 *gag-pol* expression plasmid and a vesicular stomatitis virus glycoprotein envelope expression plasmid. Vector virus produced from 293T cells was used to infect fresh MAGI target cells (Fig. 1B). Reversion mutations were detected by measuring the restored luciferase activity in the infected MAGI cells, which were either untreated or treated with antiretroviral drug. The relative mutation frequency of wild-type virus was defined as 1. The relative mutation frequencies of viruses treated with antiretroviral drugs and of viruses expressing drug-resistant RT variants were compared to this value (Materials and Methods).

Several approaches were used to validate this assay system. First, a control HIV-1 vector was constructed in which two T residues were inserted after the ATG of the *luc* gene. A mutation hot spot has been defined as a homopolymeric run of three or more nucleotides (3, 7). Therefore, the reversion mutations that occurred in this 2T vector was expected to be much lower than that when the 8T vector was used. As expected, significantly lower reversion mutations were observed when the 2T vector was used (data not shown), providing indirect evidence that the observed reversion mutations occurred during the reverse transcription process. Second, analysis of the mutation spectra at the hot spot revealed plus one, minus two, and minus one frameshift mutations. In addition, a G-to-T base substitution was also observed (Table 1). This G-to-T mutation was located at the 3′ end of the run of T's, indicating that this mutation was likely initiated by dislocation mutagenesis (4).

The mutation frequency calculated from this analysis, 4.4×10^{-3} mutations/cycle/base pair, is consistent with the previously determined HIV-1 frameshift mutation rate in a homopolymeic sequence, which is on the order of 10^{-3} (3, 28). Because only the +1 and −2 mutations can restore luciferase activity in this assay system, the relative mutation frequency of 1 correlates to 2.2×10^{-3} mutations/cycle/base pair. Based on the statistical analysis of data pooled from all control experiments, mutation frequencies are similar among all replicates, indicating that the calculated mutation frequency is representative.

Third, a control vector was constructed in which nine T residues were inserted after the start codon of the *luc* gene. This vector was designed to test whether the insertion of three amino acids would affect luciferase expression. The results revealed that the insertion of three amino acids did not significantly influence luciferase expression (data not shown). Fourth, it was observed that the detection of luciferase activity caused by reversion mutations was in the linear detection range (data not shown). Dilution of the cell lysate used in the luciferase assay resulted in a luciferase reading in the linear detection range even at high dilution points. Moreover, when the infected cell number used in the luciferase assay was increased, luciferase activity increased in a linear manner (data

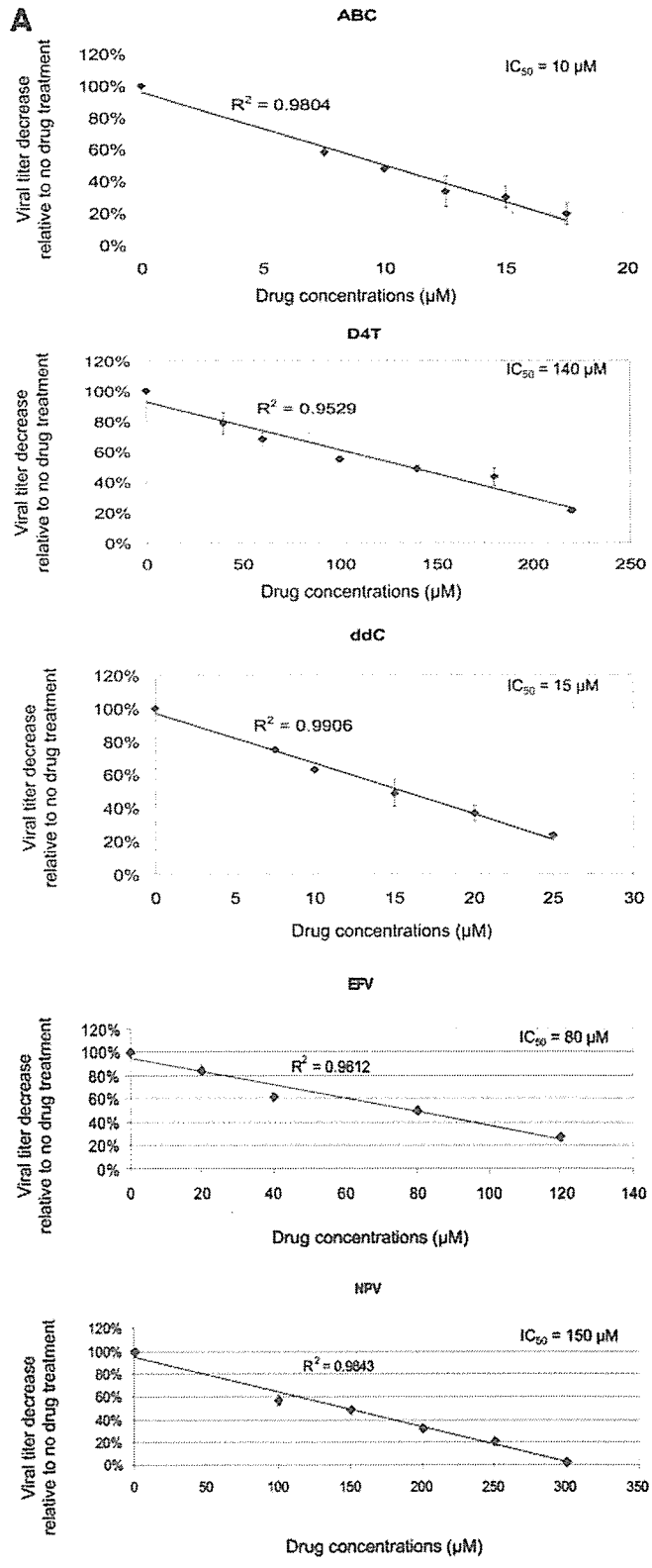

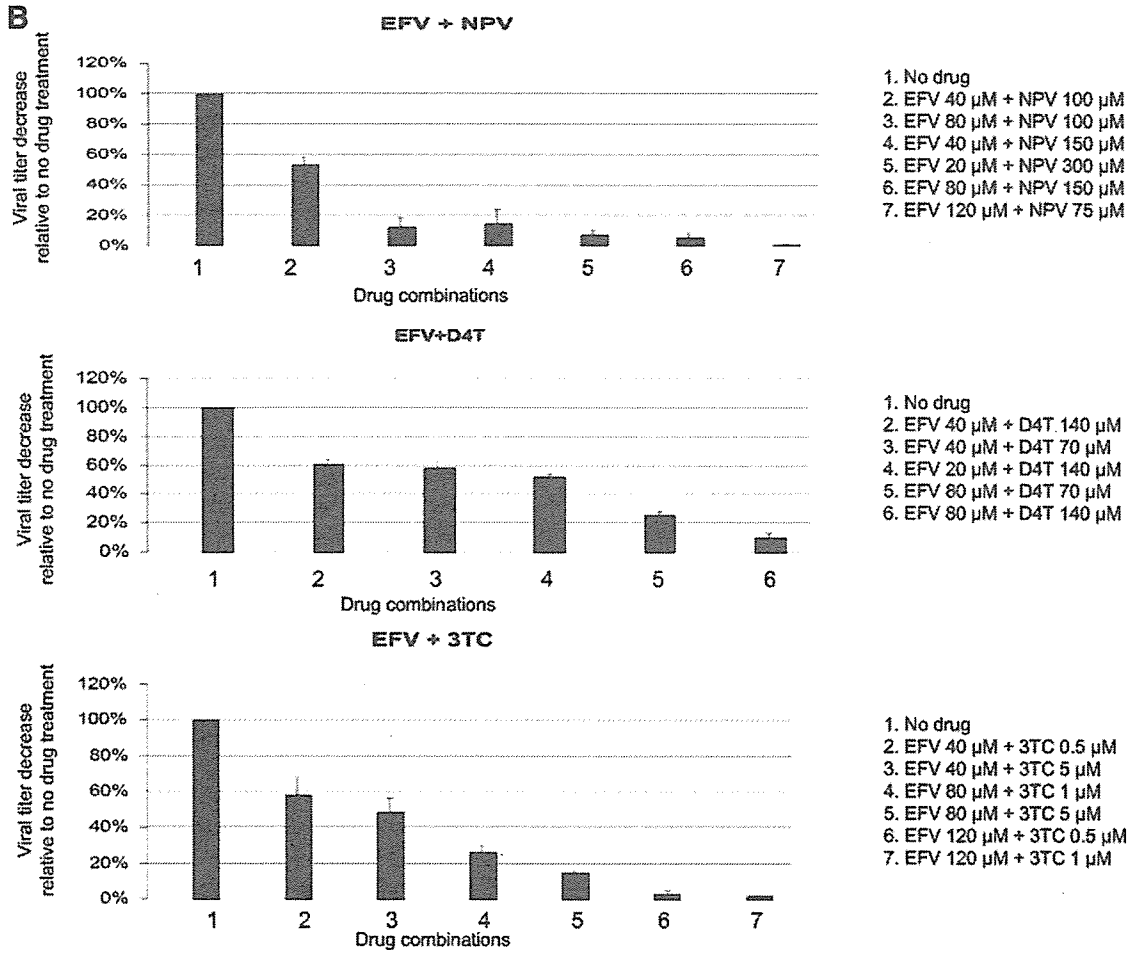

FIG. 2. Drug susceptibility assays. (A) Determination of IC_{50} values. Data from three independent experiments are shown. Virus titers from drug-treated cells are shown relative to virus titer from untreated cells (set at 100%). The absolute virus titer from untreated cells was $8.2 \times 10^5 \pm 3.5 \times 10^5$ infected cells/ml of cell-free virus stock. The IC_{50} value for lamivudine was determined previously (24). ABC, abacavir; D4T, stavudine; ddC, zalcitabine; EFV, efavirenz; NVP, nevirapine. (B) Effects of drug combinations on virus titers. The concentrations of individual drugs used in the following experiments were chosen based on the effects of the individual drugs and combined drugs on virus infectivity. Data from three independent experiments are shown. Virus titers from drug-treated cells are shown relative to the virus titer from untreated cells (set at 100%). The absolute virus titer from untreated cells was $11.5 \times 10^5 \pm 1.6 \times 10^5$ infected cells/ml of cell-free virus stock.

not shown), indicating that the increase in luciferase activity was correlated with the increase in reversion mutations that occurred during HIV-1 replication. No luciferase expression was detected in transfected cells (data not shown), indicating that the rate of reversion was very low and did not significantly contribute to the reversion frequencies observed in infected cells.

Finally, the influence of zidovudine and zidovudine-resistant RT on virus mutation frequencies was examined using this system. As shown in Table 2, zidovudine led to a 2.6-fold increase in virus mutation frequency and a zidovudine-resistant RT increased the virus mutation frequency by 2.2-fold. Replication of zidovudine-resistant virus in the presence of zidovudine led to a 6.5-fold increase in virus mutation frequencies. In comparison, it was reported that zidovudine increased the rate of +1 frameshift mutations at the run of T's in the *lacZ*α gene by twofold (24). These data provide further evidence that this new assay system behaves in a predictable manner based on previously published data using the *lacZ*α gene as a mutation target (24, 26) (Table 2).

Influence of drug-resistant RT mutants on HIV-1 mutation frequencies. In order to analyze the effects of antiretroviral drugs on virus mutation frequencies, the IC_{50} values for each

TABLE 1. Analysis of mutation spectra

Mutational class	No. of mutants/total	Mutant frequency[a] (10^{-3})
+1	1/116	1.1
−2	1/116	1.1
−1	1/116	1.1
G-to-T	1/116	1.1
Total	4/116	4.4

[a] Mutant frequency is in units of mutations/bp/cycle. The average number of relative light units for control experiments (virus replication in the presence of wild-type RT) was $6.1 \times 10^2 + 35$.

TABLE 2. Influence of zidovudine and zidovudine-resistant reverse transcriptase on HIV-1 mutant frequencies[a]

Drug	RT variant	Avg relative mutation frequency[b]	
		luc	*lacZα*
None	Wild type RT	1	1
Zidovudine		2.6 ± 0.4	7.6
None	Zidovudine resistant RT[c]	2.2 ± 0.5	4.3
Zidovudine		6.5 ± 0.3	24

[a] Data represent the average of three independent experiments. The average number of relative light units detected from infected cells for virus replication in wild-type RT was $7.0 \times 10^2 \pm 45$.

[b] Data were obtained by using the *luc* gene or *lacZα* (26) as the mutation target.

[c] The resistant RT variant contained the mutations M41L, D67N, K70R, and T215Y.

drug were first determined (Fig. 2A). Typically, cells were treated at the IC_{50} concentration of each drug to determine their influence on virus mutation frequencies. Previous studies have shown that HIV-1 replication with zidovudine-resistant RTs increased the mutation rate by as much as 4.3-fold, while replication of HIV-1 with a lamivudine-resistant RT had no significant influence on the mutation rate (24).

It was observed that only high-level zidovudine-resistant RT variants could influence the in vivo mutation rate (i.e., those containing the mutations M41L/T215Y and M41L/D67N/K70R/T215Y) (24). Moreover, it was found that combined drugs and drug-resistant RTs could further increase virus mutation frequencies (24–26). To further examine if virus mutation frequencies are influenced by drug-resistant RT variants in the presence of drugs, a series of drug-resistant RT mutants were analyzed (1, 10, 12, 20, 31, 33, 45). The mutant enzyme V75T confers resistance to the drug stavudine; Y115F confers resistance to abacavir; L74V/Y115F/M184V confers high-level resistance to abacavir and mild resistance to zalcitadine; G190A, Y318F, and K103N/Y318F confer resistance to the drugs efavirenz and nevirapine; and K103N is the most frequently observed mutation in patients treated with drug combination therapy, which includes efavirenz.

V75T was previously observed as a novel resistance mutation in cell cultures treated with stavudine. It was observed that the effect of V75T relative to wild-type RT was close to being statistically significant ($P = 0.06$). The amino acid residues that interact with the incoming deoxynucleoside triphosphate and form the deoxynucleoside triphosphate-binding site have been identified in structural studies. One substitution in the deoxynucleoside triphosphate binding site, Y115A, has been previously reported to decrease fidelity by a factor of 4 using the *lacZα* gene (14). We previously observed that the Y115A RT variant significantly increased (2.3-fold) virus mutation frequencies using one round of HIV-1 vector replication (25). Moreover, the Y115F and Y115V RT variants were found in *lacZα* cell-free fidelity assays to have slightly lower error rates than that of wild-type RT (6). In this study, we found that the Y115F RT mutant increased virus mutation frequency by only 1.20-fold, which is not significantly different from wild-type RT (Table 3) (see also below).

Cell culture selection of resistant mutants has shown that multiple mutations were required to create high levels of resistance to abacavir. One mutant, L74V/Y115F/M184V, was isolated during an in vitro passage experiment. This mutant showed a 10-fold increase in IC_{50} of abacavir, while it had a 4-fold decrease in susceptibility to zalcitabine (45). We observed that the L74V/Y115F/M184V RT mutations led to a 1.91-fold increase in HIV-1 mutation frequency and this increase is statistically significant.

Crystallographic analyses of HIV-1 RT and nonnucleoside RT inhibitor complexes have suggested that all NNRTIs occupy a hydrophobic binding pocket that is located in the palm subdomain of p66 and proximal to the polymerase active site (8, 34, 40, 41). NNRTI resistance is associated with mutations within the NNRTI binding pocket. Three single NNRTI-resistant RT mutations, K103N, G190A, and Y318F, which are all located in the NNRTI binding pocket, and one double mutation, K103N/Y318F, were tested to determine their influence on virus mutation frequencies. Clinically, the K103N mutation is the most frequently observed mutation in patients treated with efavirenz-containing therapies (1). The G190A mutation is also observed in patients treated with NNRTIs (12). The Y318F mutation is also associated with a decrease in susceptibility to NNRTIs, and viruses containing both Y318F and K103N have higher levels of drug resistance (10). As indicated in Table 3, the single RT variants K103N and G190A did not have a statistically significant impact. However, the Y318F and K103N/Y318F RT variants significantly decreased HIV-1 mutation frequencies, the latter quite substantially.

Influence of NRTIs and NRTI-resistant RT variants on virus mutation frequencies. Previous studies using the *lacZα* gene as a mutational target have indicated that NRTIs could increase virus mutation frequencies (23, 24, 26). Zidovudine increased the HIV-1 mutation rate by as much as 7.6-fold (0.4 μM) in a single round of replication, while lamivudine increased the virus mutation rate by as much as 3.4-fold (0.3 μM) (26). A dose-dependent relationship between increased drug concentration and increased virus mutation frequencies has been reported for zidovudine, lamivudine, and dideoxyinosine (23, 26, 27). The maximum increase in virus mutation frequencies in the presence of dideoxyinosine was sixfold higher than the virus mutation frequency observed during replication in the absence of drug (23).

To further investigate the impact of NRTIs on HIV-1 mutation frequencies, virus mutation frequencies were determined in the presence of other NRTIs (i.e., abacavir, stavudine, and zalcitabine) at IC_{50} concentrations. Like the other NRTIs studied previously, abacavir and stavudine led to 2.1-fold and 3.5-fold increases in virus mutation frequencies, respectively, and these effects are statistically significant. Unexpectedly, the dCTP analog zalcitabine only increased HIV-1 mutation frequencies by 1.36-fold at its IC_{50} concentration and was not statistically significant (Table 3). Based on this observation, we also tested lamivudine at its IC_{50} concentration and found that it led to a 1.20-fold increase (not significant different from no drug). At the IC_{90} concentrations of zalcitabine and lamivudine, virus mutation frequencies increased by 2.21- and 2.13-fold, respectively (Table 3), indicating that higher concentrations of zalcitabine and lamivudine are needed for these drugs to significantly influence HIV-1 mutation frequencies. This indicates that increased virus mutation frequencies occur when drug concentrations increase.

TABLE 3. Influence of HIV-1 RT variants, NRTIs, and NNRTIs on virus mutation frequencies

Class and RT variant	Drug[a] (concn, μM)	Avg relative mutation frequency[b]
Drug-resistant RT variants[c]		
Wild type		1
V75T		0.62, 0.80, 1.02
Y115F		0.85, 1.20, 1.73
L74V/Y115F/M184V		1.50, 1.91, 2.44
K103N		0.89, 1.09, 1.31
G190A		0.53, 0.83, 1.41
Y318F		0.60, 0.74, 0.91
K103N/Y318F		0.33, 0.46, 0.66
NRTIs and NRTI-resistant RT variants[d]		
Wild type	ABC	1.68, 2.14, 2.72
Y115F	ABC	2.15, 3.01, 4.24
L74V/Y115F/M184V	ABC	2.77, 3.91, 5.47
Wild type	d4T	2.60, 3.46, 4.72
V75T	d4T	1.21, 1.65, 2.18
Wild type	ddC	0.95, 1.36, 1.89
L74V/Y115F/M184V	ddC	2.37, 3.39, 4.78
Wild type	3TC	0.84, 1.20, 1.70
Wild type	ddC (15)	0.95, 1.36, 1.89
	ddC (25)	1.98, 2.21, 2.43
	3TC (1)	0.84, 1.20, 1.70
	3TC (2)	1.82, 2.13, 2.41
NNRTIs and NNRTI-resistant RT variants[e]		
Wild type	EFV	2.25, 2.69, 3.18
G190A	EFV	2.25, 3.22, 4.54
Y318F	EFV	1.70, 2.43, 3.43
K103N/Y318F	EFV	1.05, 1.47, 2.07
Wild type	NPV	2.56, 3.12, 3.80
G190A	NPV	1.88, 2.63, 3.73
Y318F	NPV	2.21, 3.09, 4.45
NNRTI and NNRTI combinations[f]		
Wild type	EFV (40)	0.98, 1.37, 1.93
	NPV (100)	1.85, 2.62, 3.76
	EFV & NPV	0.82, 2.71, 9.15
Y318F	EFV	0.95, 1.36, 1.93
	NPV	1.80, 2.64, 3.83
	EFV & NPV	0.56, 2.01, 6.99
NRTI, NNRTI, and drug-resistant RT variants[g]		
Wild type	EFV (80)	2.25, 2.69, 3.18
	d4T (140)	2.60, 3.48, 4.72
	3TC (1)	0.84, 1.20, 1.70
	EFV (80) & d4T (140)	7.28, 9.33, 11.82
	EFV (80) & 3TC (1)	2.59, 3.64, 5.21
K103N	EFV (80)	2.03, 2.83, 3.97
	d4T (140)	4.78, 7.44, 11.96
	3TC (1)	0.67, 0.97, 1.37
	EFV (80) & d4T (140)	8.28, 10.75, 12.53
	EFV (80) & 3TC (1)	1.44, 4.40, 13.11

[a] ABC, abacavir; d4T, stavudine; ddC, zalcitabine; 3TC, lamivudine; EFV, efavivenz; NPV, nevirapine.
[b] The estimated fold change (middle value) and the endpoints of the 95% confidence intervals for the fold changes are shown.
[c] The average luciferase reading for virus replication in the presence of wild-type RT was $5.5 \times 10^2 \pm 25$.
[d] The influence of NRTI and NRTI-resistant RTs on HIV-1 mutant frequencies. The average luciferase reading for virus replication in the presence of wild-type RT was $5.8 \times 10^2 \pm 26$.
[e] The influence of NNRTI and NNRTI-resistant RTs on HIV-1 mutant frequencies. The average luciferase reading for virus replication in the presence of wild-type RT $5.9 \times 10^2 \pm 32$.
[f] The influence of EFV and NPV combination and drug-resistant RT on HIV-1 mutant frequencies. Data represent the average of three to twelve independent experiments. The average luciferase reading for virus replication in the presence of wild-type RT was $5.7 \times 10^2 \pm 33$.
[g] The effects of combinations of NRTI and NNRTI and drug-resistant RT on HIV-1 mutant frequencies. The average luciferase reading for virus replication in the presence of wild-type RT was $5.9 \times 10^2 \pm 34$.

It has been shown that both RT variants and drugs together could increase virus mutation frequencies (24, 26). To further test this, selected NRTIs and drug-resistant RT variants were analyzed for their influence on virus mutation frequencies. Mutant viruses containing either the Y115F or the L74V/Y115F/M184V RT mutations were grown in the presence of abacavir at its IC_{50} concentration. Both mutations were associated with a statistically significant increase in virus mutation frequencies compared to those observed during virus replication with the wild-type RT in the presence of abacavir (Table

3). Interestingly, it was also observed that HIV-1 replication with the L74V/Y115F/M184V RT variant in the presence of zalcitabine significantly influenced HIV-1 mutation frequencies compared to that observed during virus replication with wild-type RT in the presence of zalcitabine (3.39-fold versus 1.36-fold). Similarly, in the presence of stavudine, the V75T RT variant affected virus mutation frequencies compared to wild-type RT (3.46-fold versus 1.65-fold) (Table 3).

Influence of NNRTIs and NNRTI-resistant RT variants on virus mutation frequencies. NNRTIs inhibit reverse transcription by binding to a hydrophobic pocket that is proximal to the active site of HIV-1 RT (8, 18, 34, 35, 40, 41, 43). Three NNRTIs are currently used for treatment of HIV-1 as part of combination antiretroviral therapy (39). Nothing is known about how NNRTIs affect HIV-1 mutation frequencies.

In this study, efavirenz and nevirapine and NNRTI-resistant RT variants were used to investigate how NNRTIs and NNRTI-resistant RT variants influence HIV-1 mutation frequencies. We found that efavirenz and nevirapine could increase HIV-1 mutation frequencies by 2.69 and 3.12-fold, respectively, and that these increases are statistically significant. This is the first report of NNRTIs being able to influence (increase) HIV-1 mutation frequencies. This observation surprisingly suggests that both NRTIs and NNRTIs have a similar influence on HIV-1 mutation frequencies (Table 3).

To determine the effects of NNRTI-resistant mutants on HIV-1 mutation, virus replication with NNRTI-resistant RT mutants was analyzed in the presence of these drugs. As shown in Table 3, the G190A and Y318F RT variants did not influence HIV-1 mutation frequencies compared to virus replication with wild-type RT in the presence of drug. The K103N/Y318F mutant led to an approximately 1.47-fold increase in the virus mutation frequencies in the presence of drugs compared to the 2.69-fold increase observed during virus replication with the wild-type RT in the presence of drugs.

Influence of combined drugs and HIV-1 RT variants on virus mutation frequencies. Potent antiretroviral therapy regimens typically include drugs from two of the three classes of antiretroviral drugs (NRTIs, NNRTIs, and protease inhibitors). Four two-NRTI combinations are typically used in antiretroviral therapy, i.e., zidovudine plus lamivudine, zidovudine plus dideoxyinosine, stavudine plus dideoxyinosine, and stavudine plus lamivudine (39). It has been reported that an additive increase in virus mutation frequencies was observed during virus replication in the presence of NRTI combinations (i.e., zidovudine plus dideoxyinosine, zidovudine plus lamivudine, and lamivudine plus dideoxyinosine) (23).

In this study, various combinations of drugs (NNRTI plus NNRTI and NNRTI plus NRTI) were studied for their ability to act together to influence HIV-1 mutation frequencies during virus replication. First, the drug combination of efavirenz plus nevirapine (NNRTI plus NNRTI) was tested. Based upon the effects of the individual drugs and combined drugs on virus infectivity (Fig. 2A and B) and a lack of cytotoxicity (data not shown), an efavirenz concentration of 40 μM was used along with a nevirapine concentration of 100 μM. For each drug alone, these concentrations inhibited virus replication by one-fourth. It was observed that efavirenz and nevirapine together led to an increase in the virus mutation frequency of 2.71-fold, while virus replication in the presence of efavirenz or nevirapine alone led to 1.37-fold and 2.62-fold increases in the virus mutation frequencies, respectively (Table 3).

The clinically used drug combinations of NNRTI and NRTI were then analyzed, which included efavirenz plus stavudine and efavirenz plus lamivudine. The 80 μM concentration of efavirenz was used in combination with 140 μM of stavudine or 1 μM of lamivudine, based upon the effects of the individual drugs and combined drugs on virus infectivity (Fig. 2A and B) and a lack of cytotoxicity (data not shown). As shown in Table 3, efavirenz and stavudine together could increase the HIV-1 mutation frequency by 9.33-fold, while virus replication in the presence of efavirenz or stavudine alone led to 2.69-fold and 3.46-fold increases in the virus mutation frequencies, respectively. Interestingly, the virus mutation frequency was only increased by 3.64-fold during virus replication in the presence of both efavirenz and lamivudine, which is not significantly different from the virus mutation frequency caused by efavirenz alone (Table 3). This suggests that the concentration of lamivudine was low enough to not significantly affect virus mutation frequencies.

Since there are HIV-1-infected individuals undergoing antiviral therapy who harbor viruses with drug resistance mutations, the effects of drug-resistant mutants and combined drugs on HIV-1 mutation frequencies were analyzed. It has been shown that the K103N mutant can emerge in patients treated with efavirenz-containing therapy (1), and the Y318F mutant was associated with a decrease in susceptibility to all NNRTIs (10). Therefore, the abilities of K103N and Y318F to affect the virus mutation frequencies in the presence of combined drugs were tested. In the presence of combined drugs, the K103N mutant did not have a significant influence on virus mutation frequencies compared with the mutation frequency observed for virus replication with wild-type RT in the presence of drugs except for the combination of efavirenz and stavudine, and stavudine alone (Table 3). Furthermore, virus replication with the Y318F RT variant in the presence of both efavirenz and nevirapine did not have a significant influence on HIV-1 mutation frequencies compared to virus replication with wild-type RT in the presence of both efavirenz and nevirapine (Table 3).

Influence of CRF01_AE drug-resistant RT variants on virus mutation frequencies. HIV-1 is classified into groups and subtypes based on sequences within the *gag* and *env* genes. Three separate groups, M (main), O (outlier), and N (non-M, non-O), exist. The most prevalent strains belong to group M. Group M also contains at least nine distinct subtypes or clades (A to D, F to H, and J and K), as well as several circulating recombinant forms (i.e., CRF01_AE virus) (22, 36). Much of our current understanding of HIV-1 drug resistance is derived from the studies of subtype B virus, which is the major subtype that circulates in North America and Europe. However, other subtypes, such as A, C, and E, are rapidly expanding worldwide. These variants may differ in rates of transmission, ability to cause progression to AIDS, and drug resistance profiles compared to subtype B virus (9, 15). Recently, the analysis of drug resistance profiles of recombinant RTs from subtypes CRF01_AE, B, and C demonstrated that each of these RTs possessed similar baseline sensitivity to NRTIs and NNRTIs (32).

To assess the influence of CRF01_AE mutants on HIV-1 mutation frequencies, a CRF01_AE molecular clone was used.

TABLE 4. Influence of HIV-1 CRF01_AE RT variants on virus mutation frequencies

RT variant	Mutation(s)[a]	Drug resistance phenotype[b]	Avg relative mutation frequency[c]
93JP-NH1	None	None	1
CRF01_AE mt-1	M41L, L210W, T215Y	AZT (mild)	0.80, 0.88, 0.96
CRF01_AE mt-2	Insertion[d]	3TC (weak)	0.68, 0.92, 1.16
CRF01_AE mt-5	Insertion + AZT[e]	AZT (high), 3TC (mild), d4T (weak), ddI (weak)	0.76, 0.86, 0.96
CRF01_AE mt-6	Insertion[d] + AZT[e] + T69I	AZT (high), 3TC (high), d4T (mild), ddI (mild), ddC (weak)	0.81, 0.87, 0.93
CRF01_AE mt-7	Insertion[d] + AZT[e] + T69I and others[f]	AZT (high), 3TC (high), d4T (mild), ddI (mild), ddC (weak)	0.59, 0.69, 0.79

[a] The insertion is an 11-amino-acid insertion located between codons 67 and 68 in the β3–β4 loop coding region of the RT gene.
[b] See Table 3, footnote *a*.
[c] Endpoints of 95% confidence intervals and the sample mean are presented. The average number of relative light units for virus replication in the presence of wild-type RT was $6.3 \times 10^2 \pm 38$.
[d] Reverse transcriptase variants had an 11-amino-acid insertion between codons 67 and 68 in the β3-β4 loop coding region. The amino acid insertion was NIHGGRDQGPA.
[e] Reverse transcriptase variants with the zidovudine (AZT) resistance mutations M41L, D67N, K70R, L210W, and T215Y.
[f] The other mutations in reverse transcriptase included D6E, K39E, E43K, T69I, G196E, T200R, and L228R.

This molecular clone was constructed from the 93JP-NH1 virus isolate (p93JP-NH1). Based upon previous studies, RT variants that confer multiple-drug resistance were introduced by site-directed mutagenesis (38). All CRF01_AE RT variants except CRF01_AE-mt1 have a β3-β4-loop-insertion mutation at a similar position seen in subtype B viruses with multiple NRTI resistance. The HIV-1 isolates with the insertion mutation predominated in a patient treated with multiple NRTIs. The RT variants and their drug resistance profiles are listed in Table 4. As shown in Table 4, the p93JP-NH1 RT influenced the virus mutation frequencies at a level comparable to wild-type subtype B RT. Only one CRF01_AE mutation that confers high levels of multi-nucleoside analog drug resistance had a significant influence on HIV-1 mutation frequencies (i.e., CRF01_AE mt-7).

Structural analysis. To help determine the underlying molecular mechanisms by which drugs and drug resistance mutations alter the mutation frequency of HIV-1 subtype B and CRF01_A/E, we have conducted structural analyses by integrating HIV-1 RT structure-function information into the following two basic models for mutation. One basic model explains how misalignments of the primer-template are initiated, in which nucleotide misinsertion into the catalytic site plays a key role in inducing template-primer slippage for −1, −2, and +1 frameshift mutations and dislocation mutagenesis of HIV-1 RT (5). Studies of frameshift error rates with various polymerases, including HIV-1 RT, have supported this model (19). The other model explains how high levels of DNA replication fidelity are generated during the catalytic cycle of the various polymerases, in which there are at least two critical check points for the nucleotide selection in the early phase: check of base pair geometry at initial binding of substrate and check of steric hindrance during finger-domain rotation that locates the substrate at the catalytic site (19). Although the previous structural (11, 37) and kinetic (16, 35) studies with HIV-1 RT are consistent with this induced-fit model, the initial substrate binding site on RT to evaluate nucleotide selection fidelity remains to be determined.

To assess the initial binding site of deoxynucleoside triphosphates or NRTIs with HIV-1 RT, we have conducted computer-assisted docking simulations by using the crystal structure of the RT-template-primer complex (PDB code 1N5Y) (37) as a template for nucleotide docking. The crystal structure represents a fingers-open configuration at the posttranslocation stage during the catalytic cycle of RT, which is theoretically competent for de novo substrate binding. As shown in Fig. 3, dATP, which is the complementary substrate for the 1N5Y template DNA, was predicted to bind the site along the β3-β4 loops of the p66 fingers subdomain. Other deoxynucleoside triphosphate and deoxynucleoside triphosphate analogs such as zidovudine triphosphate and stavudine triphosphate shared the same binding site with the dATP (data not shown). Interestingly, the predicted initial binding position of the nucleotides was distinct from the position of dTTP at the catalytic site in the RT crystal structure of the fingers-closed configuration (11) and is consistent with the position to initiate effectively the base pair formation and fingers rotation in the induced-fit model. The position was also in agreement with the biochemical mode of NRTI inhibition, competitive inhibition, shown by kinetics studies. Furthermore, the position was analogous to that of other polymerases determined by x-ray crystallography (13, 21, 44, 46).

In the crystal structure, positively charged amino acids are responsible for the initial binding of substrates (13, 21, 44, 46). Consistently, K65 and R72 in the β3 and β4 loops of HIV-1 RT correspond to those amino acids that are interacting with the deoxynucleoside triphosphate. The NRTI docking model with the information of the NNRTI binding site (18, 43) and the two basic models described above help explain the changes in mutation frequencies observed in the present study and in previous studies (25).

DISCUSSION

Previous studies using the *lacZα* peptide gene as a mutation target have indicated that both antiretroviral drugs and drug-resistant RTs can increase HIV-1 mutation frequencies (24–26). In this study, we have analyzed virus mutation frequencies in a single round of replication with an HIV-1 vector containing the *luc* gene. This vector was designed to specifically detect frameshift mutations based on previous in vitro and in vivo studies (3, 4, 7, 24, 28). The advantages of this new high-

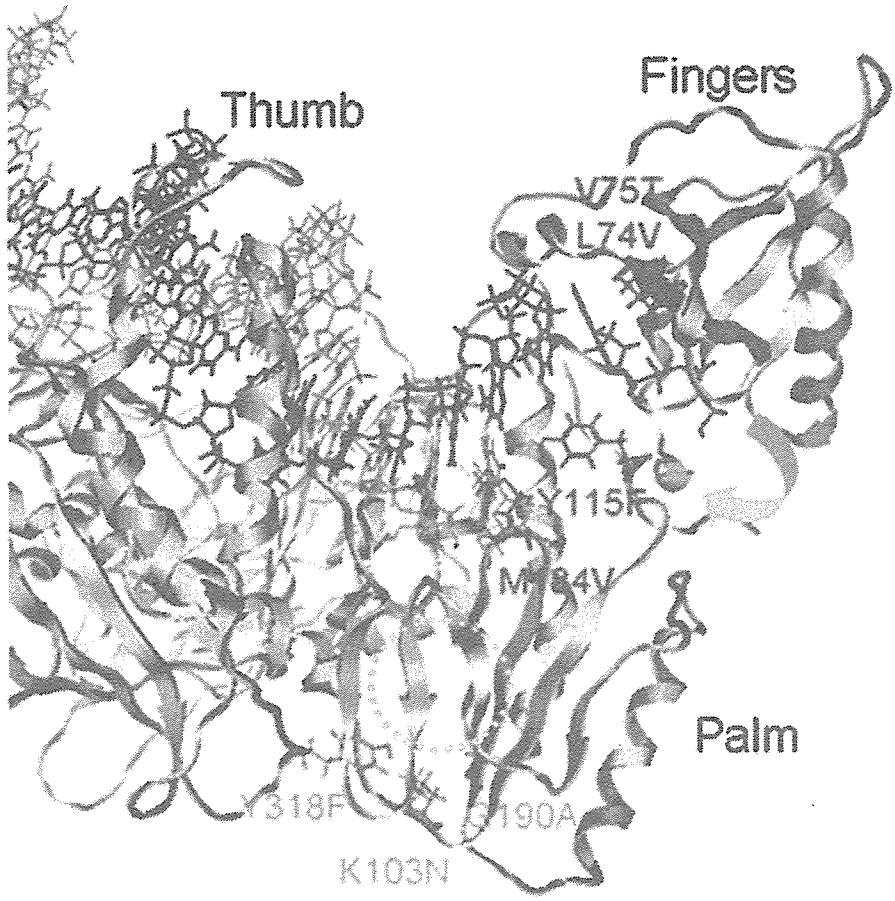

FIG. 3. Structural model of the active site of the HIV-1 reverse transcriptase p66 subunit open configuration with newly bound dATP, primer, and template. The three-dimensional model that simulates de novo substrate binding to RT at the posttranslocation stage during the catalytic cycle was constructed by docking dATP onto the crystal structure (PDB code 1N5Y) (37) by using the molecular operating environment. The incoming dATP (blue sticks) in the open ternary complex is bound to the initial binding site along the β3-β4 loops in the p66 fingers subdomain. The ribbon represents the backbone of HIV-1 RT. The DNA template and primer are shown in magenta sticks and green sticks, respectively. The NRTI resistance mutations and NNRTI resistance mutations analyzed in this study are shown in pink and orange, respectively. A dotted cyan circle indicates the site for NNRTI binding (18, 43). The cyan arrow indicates the rotation of the fingers subdomain following substrate incorporation at the catalytic site of the enzyme (11).

throughput assay system are that it allows the rapid assessment of the influence of drugs and drug-resistant RT variants on HIV-1 mutation frequencies and the sensitivity of the luciferase assay allows detection of reversion mutations in relatively small samples.

The virus mutation frequencies measured are representative based on previous observations made of frameshift mutations created in the presence and absence of drugs or drug-resistant HIV-1 using *lacZ*α (26) and provide a good model for identifying mutations that occur during virus replication. However, in certain instances, this new assay may underestimate mutation frequency change because this HIV-1 vector was designed to detect only frameshift mutations and not the entire spectra of mutations. One case in point is when the influence of zidovudine and zidovudine-resistant RT mutants on virus mutation frequencies was compared. In this comparison, zidovudine and zidovudine-resistant RT led to a lower mutation frequency using *luc* versus the *lacZ*α reporter (Table 2), indicating that there was an underestimate of the effects of drugs and drug-resistant RTs on virus mutation frequencies. However, this new system can quickly assess the influence of drugs and drug-resistant RT mutations on HIV-1 mutation frequencies during virus replication that could subsequently be analyzed in greater detail using the *lacZ*α system.

Drug-resistant RTs influence HIV-1 mutation frequencies. Several drug-resistant RT variants were observed to significantly alter HIV-1 mutation frequencies. First, the RT variant L74V/Y115F/M184V, which confers high resistance to abacavir, led to a significant increase in virus mutation frequencies, which is in contrast to the individual mutations, which do not lead to significant differences compared to wild-type RT. Second, the NNRTI-resistant RT variants Y318F and K103N/Y318F led to significant decreases in virus mutation frequencies. This is the first report that NNRTI-resistant RT can alter HIV mutation frequencies. Third, the CRF01_AE RT variant CRF01_AE mt-7, which confers high levels of multi-nucleoside analog drug resistance, led to a significant decrease in virus mutation frequencies. Our previous work found that only high-level zidovudine-resistant RT variants could influence the in vivo mutation rate. Therefore, our data suggests that increased

drug resistance correlates with altered virus mutation frequencies.

It is not clear how the mutations that confer NNRTI resistance influence virus mutation frequencies. These residues are located within the hydrophobic NNRTI-binding pocket, which could cause conformational changes in the pocket. Therefore, it is possible that NNRTI-resistant RT mutants could indirectly affect the conformation of the HIV-1 RT active site and subsequently influence HIV-1 mutation frequencies. Biochemical studies of how NNRTI-resistant RT mutants influence misincorporation, mismatch extension, and processivity of RT would also help us to understand how NNRTI-resistant RTs affect viral mutagenesis.

NRTIs and NNRTIs can increase HIV-1 mutation frequencies. The observation that abacavir, stavudine, and zalcitabine influence HIV-1 mutation frequencies indicates that the approved NRTIs currently used in drug therapy can increase virus mutation frequencies. Current studies are being directed at understanding the molecular basis for how NRTIs influence HIV-1 mutagenesis. These data suggest that NNRTIs and NRTIs have similar effects on HIV-1 mutagenesis. The mechanism by which NNRTIs increase HIV-1 mutation frequencies is presently unknown. One hypothesis is that the conformational change caused by NNRTIs binding noncatalytically to RT may affect enzyme fidelity.

Crystallographic studies have shown that NNRTIs cause a repositioning of the three-stranded β-sheet in the p66 subunit (containing the catalytic aspartic acid residues 110, 185, and 186), and there is a striking similarity between the actual conformations of the three-stranded β-sheet in the drug-bound p66 conformation and in the inactive p51 conformation (8). This suggests that the NNRTIs inhibit HIV-1 RT by locking the active catalytic site in an inactive conformation, reminiscent of the conformation observed in the inactive p51 subunit (8). This conformational change has a dramatic effect on the rate of the chemical step (transfer of deoxynucleoside monophosphate to the end of the primer molecule) of polymerization (35). Hence, the conformational change of the RT active site caused by NNRTIs could influence either nucleotide selectivity or RT processivity, which would lead to lower fidelity of NNRTI-bound RT compared to wild-type RT.

The effects of combined drugs (NNRTI plus NNRTI) on HIV-1 mutation frequencies were analyzed. In general, the virus mutation frequencies observed in the presence of combined drugs were significantly increased compared to that observed in the presence of the individual drugs. This indicates that these two NNRTIs can act together in an additive manner to further increase HIV-1 mutation frequencies. The clinical use of drug combinations of NNRTI plus NRTI, such as efavirenz plus stavudine or efavirenz plus lamivudine, were also examined and found to act together in an additive manner. This is the first report which shows that an NRTI-NNRTI combination could further increase HIV-1 mutation frequencies. Given that potent antiretroviral therapy typically includes two or three RT inhibitors, the combined effects of RT inhibitors on HIV-1 mutation frequencies may be clinically relevant.

Potential mechanisms for NRTI resistance mutations and NRTI-mediated changes in HIV-1 mutation frequency. First, the docking model in Fig. 3 predicts that mutations near the β3-β4 loop alter the base pair geometry upon initial substrate binding, leading to changes in the frequency of correct substrate incorporation at the catalytic site. Thus, NRTI resistance mutations on the fingers subdomain that had evolved to play roles in better rejection of incorrect substrate will generally decrease the frequency of misinsertion and thereby frameshift mutation, as observed in this study (Table 3 and Fig. 3, V75T) and previous studies (25). The L74V mutation on the β3-β4 loop is unique in that it causes virus hypersensitivity to zidovudine (42). Such a mutation may decrease the fidelity of geometric selection of the correct substrate, leading to an increase in mutation frequency.

Second, the model predicts that mutations along the interface of the palm subdomain of RT alter the nature of steric hindrance during the movement of the fingers and subsequent proper positioning of substrate at the catalytic site, resulting in an altered mutation frequency. For example, the Y115A mutations will induce less restricted rotation of the fingers subdomain because of the loss of the aromatic ring and the hydroxyl group at the side chain of the phenylalanine, respectively, leading to an increase in the probability of misinsertion-mediated mutations, as was observed in the previous study (25). Third, mutations around the catalytic site that reduce the rate of polymerization will cause increased susceptibility to the ATP-mediated excision reaction for the removal of a residue at the primer 3′ end (29, 30), leading to an increase in fidelity of DNA replication.

The docking model also explains why various NRTIs can increase HIV-1 mutation frequencies. The experimental conditions used in the present studies result in relatively high concentrations of the intracellular triphosphate form of the NRTI (NRTI-triphosphate), which is a potent competitive inhibitor of deoxynucleoside triphosphate as suggested in both the present and previous studies. This in turn will result in the reduction of frequency in correct deoxynucleoside triphosphate incorporation into the catalytic site, provided that the NRTI-triphosphate-template geometry is similar to that of the correct deoxynucleoside triphosphate-template base pair, leading to an increase in misinsertion and frameshift mutation frequencies. For example, abacavir-triphosphate, as a dGTP analogue, will become a competitor of the correct substrate dATP in the present system, because abacavir-triphosphate has structural similarity to dATP in that it has a purine base, as dATP has. Similarly, stavudine triphosphate will become a competitor of dATP incorporation, because the stavudine triphosphate can make two hydrogen bonds with the T template after initial binding. However, dCTP analogs such as lamivudine and zalcitabine will be less efficient competitors because of the lack of favorable hydrogen bond formation with thymidine and because of the similarity of base structure. This differential competition for each NRTI-triphosphate in turn will lead to the differential reduction in frequency of correct substrate (dATP) incorporation into the catalytic site, leading to a differential increase in mutation frequency, as seen in the present study (Table 3).

Potential mechanisms for NNRTI and NNRTI resistance mutation-mediated changes in HIV-1 mutation frequency. The induced-fit model and the activity of ATP-mediated excision (29, 30) suggest a potential mechanism to explain the NNRTI-mediated increase in mutation frequency. NNRTIs, as allosteric inhibitors of RT activity, inhibit the above ATP-mediated

excision reaction, probably by locking the structure of the RT active center and inhibiting ATP binding to RT (2). Therefore it is possible that the binding of an NNRTI to RT suppresses ATP binding to RT, leading to suppression of ATP-mediated RT changes for increasing the fidelity of substrate selection, such as in the excision reaction. This in turn will increase misinsertion-mediated mutation frequencies. On the other hand, NNRTI resistance mutations will reverse the suppression effects of NNRTI in a resistance level-dependent manner, which will partially restore the ATP-binding activity and its function for higher fidelity (as observed in Table 3). Further studies using this newly developed high-throughput assay along with structure-function analysis of HIV-1 RT will help in our understanding of what influences HIV-1 mutagenesis in cells.

ACKNOWLEDGMENT

This work was supported by National Institutes of Health grant GM56615.

REFERENCES

1. **Bacheler, L. T., E. D. Anton, P. Kudish, D. Baker, J. Bunville, K. Krakowski, L. Bolling, M. Aujay, X. V. Wang, D. Ellis, M. F. Becker, A. L. Lasut, H. J. George, D. R. Spalding, G. Hollis, and K. Abremske.** 2000. Human immunodeficiency virus type 1 mutations selected in patients failing efavirenz combination therapy. Antimicrob. Agents Chemother. **44**:2475–2484.
2. **Basavapathruni, A., C. M. Bailey, and K. S. Anderson.** 2004. Defining a molecular mechanism of synergy between nucleoside and nonnucleoside AIDS drugs. J. Biol. Chem. **279**:6221–6224.
3. **Bebenek, K., J. Abbotts, J. D. Roberts, S. H. Wilson, and T. A. Kunkel.** 1989. Specificity and mechanism of error-prone replication by human immunodeficiency virus-1 reverse transcriptase. J. Biol. Chem. **264**:16948–16956.
4. **Bebenek, K., J. Abbotts, S. H. Wilson, and T. A. Kunkel.** 1993. Error-prone polymerization by HIV-1 reverse transcriptase. Contribution of template-primer misalignment, miscoding, and termination probability to mutational hot spots. J. Biol. Chem. **268**:10324–10334.
5. **Bebenek, K., J. D. Roberts, and T. A. Kunkel.** 1992. The effects of dNTP pool imbalances on frameshift fidelity during DNA replication. J. Biol. Chem. **267**:3589–3596.
6. **Boyer, P. L., and S. H. Hughes.** 2000. Effects of amino acid substitutions at position 115 on the fidelity of human immunodeficiency virus type 1 reverse transcriptase. J. Virol. **74**:6494–6500.
7. **Burns, D. P., and H. M. Temin.** 1994. High rates of frameshift mutations within homo-oligomeric runs during a single cycle of retroviral replication. J. Virol. **68**:4196–4203.
8. **Esnouf, R., J. Ren, C. Ross, Y. Jones, D. Stammers, and D. Stuart.** 1995. Mechanism of inhibition of HIV-1 reverse transcriptase by nonnucleoside inhibitors. Struct. Biol. **2**:303–308.
9. **Essex, M.** 1999. Human immunodeficiency viruses in the developing world. Adv. Virus Res. **53**:71–88.
10. **Harrigan, P. R., M. Salim, D. K. Stammers, B. Wynhoven, Z. L. Brumme, P. McKenna, B. Larder, and S. D. Kemp.** 2002. A mutation in the 3′ region of the human immunodeficiency virus type 1 reverse transcriptase (Y318F) associated with nonnucleoside reverase transcriptase inhibitor resistance. J. Virol. **76**:6836–6840.
11. **Huang, H., R. Chopra, G. L. Verdine, and S. C. Harrison.** 1998. Structure of a covalently trapped catalytic complex of HIV-1 reverse transcriptase: implications for drug resistance. Science **282**:1669–1675.
12. **Huang, W., A. Gamarnik, K. Limoli, C. J. Petropoulos, and J. M. Whitcomb.** 2003. Amino acid substitutions at position 190 of human immunodeficiency virus type 1 reverse transcriptase increase susceptibility to delavirdine and impair virus replication. J. Virol. **77**:1512–1523.
13. **Johnson, S. J., J. S. Taylor, and L. S. Beese.** 2003. Processive DNA synthesis observed in a polymerase crystal suggests a mechanism for the prevention of frameshift mutations. Proc. Natl. Acad. Sci. USA **100**:3895–3900.
14. **Jonckheere, H., E. De Clercq, and J. Anne.** 2000. Fidelity analysis of HIV-1 reverse transcriptase mutants with an altered amino-acid sequence at residues Leu74, Glu89, Tyr115, Tyr183 and Met184. Eur. J. Biochem. **267**:2658–2665.
15. **Kanki, P. J., D. J. Hamel, J. L. Sankale, C. Hsieh, I. Thior, F. Barin, S. A. Woodcock, A. Gueye-Ndiaye, E. Zhang, M. Montano, T. Siby, R. Marlink, I. NDoye, M. E. Essex, and, S. MBoup.** 1999. Human immunodeficiency virus type 1 subtypes differ in disease progression. J. Infect. Dis. **179**:68–73.
16. **Kati, W. M., K. A. Johnson, L. F. Jerva, and K. S. Anderson.** 1992. Mechanism and fidelity of HIV reverse transcriptase. J. Biol. Chem. **267**:25988–25997.
17. **Kimpton, J., and M. Emerman.** 1992. Detection of replication-competent and pseudotyped human immunodeficiency virus with a sensitive cell line on the basis of activation of an integrated beta-galactosidase gene. J. Virol. **66**:2232–2239.
18. **Kohlstaedt, L. A., J. Wang, J. M. Friedman, P. A. Rice, and T. A. Steitz.** 1992. Crystal structure at 3.5 A resolution of HIV-1 reverse transcriptase complexed with an inhibitor. Science **256**:1783–1790.
19. **Kunkel, T. A., and K. Bebenek.** 2000. DNA replication fidelity. Annu. Rev. Biochem. **69**:497–529.
20. **Lacey, S. F., and B. A. Larder.** 1994. Novel mutation (V75T) in human immunodeficiency virus type 1 reverse transcriptase confers resistance to 2′,3′-didehydro-2′,3′-dideoxythymidine in cell culture. Antimicrob. Agents Chemother. **38**:1428–1432.
21. **Li, Y., Y. Kong, S. Korolev, and G. Waksman.** 1998. Crystal structures of the Klenow fragment of Thermus aquaticus DNA polymerase I complexed with deoxyribonucleoside triphosphates. Protein Sci. **7**:1116–1123.
22. **Louwagie, J., W. Janssens, J. Mascola, L. Heyndrickx, P. Hegerich, G. van der Groen, F. E. McCutchan, and D. S. Burke.** 1995. Genetic diversity of the envelope glycoprotein from human immunodeficiency virus type 1 isolates of African origin. J. Virol. **69**:263–271.
23. **Mansky, L. M.** 2003. Mutagenic outcome of combined antiviral drug treatment during human immunodeficiency virus type 1 replication. Virology **307**:116–121.
24. **Mansky, L. M., and L. C. Bernard.** 2000. 3′-Azido-3′-deoxythymidine (zidovudine) and AZT-resistant reverse transcriptase can increase the in vivo mutation rate of human immunodeficiency type 1. J. Virol. **74**:9532–9539.
25. **Mansky, L. M., E. Le Rouzic, S. Benichou, and L. C. Gajary.** 2003. Influence of reverse transcriptase variants, drugs, and Vpr on human immunodeficiency virus type 1 mutation frequencies. J. Virol. **77**:2071–2080.
26. **Mansky, L. M., D. K. Pearl, and L. C. Gajary.** 2002. Combination of drugs and drug-resistant reverse transcriptase results in a multiplicative increase of human immunodeficiency virus type 1 mutation frequencies. J. Virol. **76**: 9253–9259.
27. **Mansky, L. M., S. Preveral, L. Selig, R. Benarous, and S. Benichou.** 2000. The interaction of Vpr with uracil DNA glycosylase modulates the human immunodeficiency virus type 1 in vivo mutation rate. J. Virol. **74**:7039–7047.
28. **Mansky, L. M., and H. M. Temin.** 1995. Lower in vivo mutation rate of human immunodeficiency virus type 1 than that predicted from the fidelity of purified reverse transcriptase. J. Virol. **69**:5087–5094.
29. **Meyer, P. R., S. E. Matsuura, A. G. So, and W. A. Scott.** 1998. Unblocking of chain-terminated primer by HIV-1 reverse transcriptase through a nucleotide-dependent mechanism. Proc. Natl. Acad. Sci. USA **95**:13471–13476.
30. **Meyer, P. R., S. E. Matsuura, A. A. Tolun, I. Pfeifer, A. G. So, J. W. Mellors, and W. A. Scott.** 2002. Effects of specific zidovudine resistance mutations and substrate structure on nucleotide-dependent primer unblocking by human immunodeficiency virus type 1 reverse transcriptase. Antimicrob. Agents Chemother. **46**:1540–1545.
31. **Pelemans, H., R. M. Esnouf, H. Jonckheere, E. De Clercq, and J. Balzarini.** 1998. Mutational analysis of Tyr-318 within the non-nucleoside reverse transcriptase inhibitor binding pocket of human immunodeficiency virus type 1 reverse transcriptase. J. Biol. Chem. **273**:34234–34239.
32. **Quan, Y., B. G. Brenner, R. G. Marlink, M. Essex, T. Kurimura, and M. A. Wainberg.** 2003. Drug resistance profiles of recombinant reverse transcriptases from human immunodeficiency virus type 1 subtypes A/E, B, and C. AIDS Res. Hum. Retroviruses **19**:743–753.
33. **Ray, A. S., A. Basavapathruni, and K. S. Anderson.** 2002. Mechanistic studies to understand the progressive development of resistance in human immunodeficiency virus type 1 reverse transcriptase to abacavir. J. Biol. Chem. **277**:40479–40490.
34. **Ren, J., R. Esnouf, E. Garman, D. Somers, C. Ross, I. Kirby, J. Keeling, G. Darby, Y. Jones, D. Stuart, and D. Stammers.** 1995. High resolution structures of HIV-1 RT from four RT-inhibitor complexes. Struct. Biol. **2**:293–302.
35. **Rittinger, K., G. Divita, and R. S. Goody.** 1995. Human immunodeficiency virus reverse transcriptase substrate-induced conformational changes and the mechanism of inhibition by nonnucleoside inhibitors. Proc. Natl. Acad. Sci. USA **92**:8046–8049.
36. **Robertson, D. L., J. P. Anderson, J. A. Bradac, J. K. Carr, B. Foley, R. K. Funkhouser, F. Gao, B. H. Hahn, M. L. Kalish, C. Kuiken, G. H. Learn, T. Leitner, F. McCutchan, S. Osmanov, M. Peeters, D. Pieniazek, M. Salminen, P. M. Sharp, S. Wolinsky, and B. Korber.** 2000. HIV-1 nomenclature proposal. Science **288**:55–56.
37. **Sarafianos, S. G., A. D. Clark, Jr., K. Das, S. Tuske, J. J. Birktoft, P. Ilankumaran, A. R. Ramesha, J. M. Sayer, D. M. Jerina, P. L. Boyer, S. H. Hughes, and E. Arnold.** 2002. Structures of HIV-1 reverse transcriptase with pre- and post-translocation AZTMP-terminated DNA. EMBO J. **21**:6614–6624.
38. **Sato, H., Y. Tomita, K. Ebisawa, A. Hachiya, K. Shibamura, T. Shiino, R. Yang, M. Tatsumi, K. Gushi, H. Umeyama, S. Oka, Y. Takebe, and Y. Nagai.** 2001. Augmentation of human immunodeficiency virus type 1 subtype E (CRF01_AE) multiple-drug resistance by insertion of a foreign 11-amino-acid fragment into the reverse transcriptase. J. Virol. **75**:5604–5613.

39. **Shafer, R. W., and D. A. Vuitton.** 1999. Highly active antiretroviral therapy (HAART) for the treatment of infection with human immunodeficiency virus type 1. Biomed. Pharmacother. **53**:73–86.
40. **Smerdon, S. J., J. Jager, J. Wang, L. A. Kohlstaedt, A. J. Chirino, J. M. Friedman, P. A. Rice, and T. A. Steitz.** 1994. Structure of the binding site for nonnucleoside inhibitors of the reverse transcriptase of human immunodeficiency virus type 1. Proc. Natl. Acad. Sci. USA **91**:3911–3915.
41. **Spence, R. A., W. M. Kati, K. S. Anderson, and K. A. Johnson.** 1995. Mechanism of inhibition of HIV-1 reverse transcriptase by nonnucleoside inhibitors. Science **267**:988–993.
42. **St Clair, M. H., J. L. Martin, G. Tudor-Williams, M. C. Bach, C. L. Vavro, D. M. King, P. Kellam, S. D. Kemp, and B. A. Larder.** 1991. Resistance to ddI and sensitivity to AZT induced by a mutation in HIV-1 reverse transcriptase. Science **253**:1557–1559.
43. **Tantillo, C., J. Ding, A. Jacobo-Molina, R. G. Nanni, P. L. Boyer, S. H. Hughes, R. Pauwels, K. Andries, P. A. Janssen, and E. Arnold.** 1994. Locations of anti-AIDS drug binding sites and resistance mutations in the three-dimensional structure of HIV-1 reverse transcriptase. Implications for mechanisms of drug inhibition and resistance. J. Mol. Biol. **243**:369–387.
44. **Temiakov, D., V. Patlan, M. Anikin, W. T. McAllister, S. Yokoyama, and D. G. Vassylyev.** 2004. Structural basis for substrate selection by t7 RNA polymerase. Cell **116**:381–391.
45. **Tisdale, M., T. Alnadaf, and D. Cousens.** 1997. Combination of mutations in human immunodeficiency virus type 1 reverse transcriptase required for resistance to the carbocyclic nucleoside 1592U89. Antimicrob. Agents Chemother. **41**:1094–1098.
46. **Yin, Y. W., and T. A. Steitz.** 2004. The structural mechanism of translocation and helicase activity in T7 RNA polymerase. Cell **116**:393–404.

JOURNAL OF VIROLOGY, May 2005, p. 5996–6004 Vol. 79, No. 10
0022-538X/05/$08.00+0 doi:10.1128/JVI.79.10.5996–6004.2005

Amino Acid 36 in the Human Immunodeficiency Virus Type 1 gp41 Ectodomain Controls Fusogenic Activity: Implications for the Molecular Mechanism of Viral Escape from a Fusion Inhibitor

Masanobu Kinomoto,[1,3] Masaru Yokoyama,[2] Hironori Sato,[2] Asato Kojima,[1] Takeshi Kurata,[1] Kazuyoshi Ikuta,[3] Tetsutaro Sata,[1] and Kenzo Tokunaga[1]*

Department of Pathology[1] and Division of Molecular Genetics,[2] National Institute of Infectious Diseases, Tokyo 162-8640, and Department of Virology, Research Institute for Microbial Diseases, Osaka University, Osaka 565-0871,[3] Japan

Received 29 October 2004/Accepted 6 January 2005

We have previously described a human immunodeficiency virus type 1 (HIV-1) proviral clone, pL2, derived from defective viral particles with higher fusogenicity than the prototypic NL4-3 virus. In this study, we attempted to determine the region that confers the enhanced fusion activity by creating envelope recombinants between pL2 and pNL4-3, as well as point mutants based on pNL4-3. The results indicate that amino acid 36 of gp41 is key for the fusogenic activity and infectivity enhancement and that glycine 36 (36G) of gp41 in pL2 is conserved in nearly all HIV-1 isolates except for pNL4-3. The mutation 36G→D in a primary-isolate-derived Env decreased syncytium-forming activity and infectivity. The assays for cell-cell fusion and viral binding suggested that the enhanced fusion mediated by the 36D→G mutation is not due to increased binding efficiency but is directly due to actual enhancement of viral fusion activity. Interestingly, this amino acid position is exactly equivalent to that at which the mutation of HIV-1 isolates that have escaped from a fusion inhibitor, enfuvirtide (T-20), has been frequently observed. The correlation between these previous findings and our findings was suggested by structural analysis. Our finding, therefore, has implications for a molecular basis of the viral escape from this drug.

The human immunodeficiency virus type 1 (HIV-1) envelope glycoprotein (Env), which determines viral tropism, is initially synthesized as a single polypeptide precursor, gp160, forming trimers (46). Subsequently, this Env precursor is cleaved proteolytically into a heavily glycosylated surface subunit known as gp120 and a transmembrane subunit known as gp41, which are associated by noncovalent bonds in an oligomeric structure on the surface of the virion (10, 18, 31). On the target cell surface, the gp120 surface protein binds to CD4 and a coreceptor, leading to a conformational change in gp120 that alters gp120-gp41 interactions (23, 47). This binding event triggers membrane fusion, which requires functions of gp41 ectodomain. The gp41 ectodomain contains a hydrophobic amino-terminal fusion peptide, followed by an amino-terminal and carboxy-terminal leucine/isoleucine heptad repeat domain with a helical structure (N-peptide helix and C-peptide helix, respectively) (3, 6, 26, 36, 43). Fusion is first induced by insertion of the fusion peptide at the amino terminus of gp41 into the host cell membrane, after which this region is brought into close proximity to the transmembrane domain of gp41. This is attained via the fusion-active conformation of a coiled-coil structure composed of internal triple-stranded N-peptide helices paired with antiparallel outer C-peptide helices packed along hydrophobic grooves, thus forming a six-helix bundle (7, 43).

The fusion inhibitor enfuvirtide (also known as T-20), a peptide based on the sequence of the C-peptide helix in gp41, blocks formation of the six-helix bundle and thus prevents membrane fusion (8, 27, 45). A mutation in the N-peptide helix of gp41, specifically, an aspartic acid substitution for glycine at position 36, which was selected both in vitro (24, 35, 40) and in vivo (42), affects viral sensitivity to T-20, presumably by altering the affinity of T-20 for the N-peptide helix.

We have previously reported that an established cell line, L-2, derived from MT-4 cells surviving after in vitro acute-phase infection with an MT-4/MOLT-4 cell-propagated LAI strain, produces highly fusogenic but replication-defective HIV-1 particles (20). The L-2-produced viruses are peculiar, as the morphology of the viral particles is doughnut shaped since the protease gene is mutated and in that the virions harbor a robust activity to induce syncytia despite lacking infectivity (16, 32). To characterize the L-2-derived viruses, we generated a full-length infectious DNA clone, pL2, using proviral DNA extracted from L-2 cells. By performing a chimeric analysis between pL2 and pNL4-3, we found that pL2-derived regions, including *env*, induce enhanced syncytium formation as expected (21).

In this study, we further sought to determine the region that conferred the fusogenic activity at the amino acid level, by creating *env* recombinants between pL2 (or its parent pLAI) and pNL4-3, and several point mutants based on pNL4-3. The results demonstrate that amino acid 36 of gp41 is a key deter-

* Corresponding author. Mailing address: Department of Pathology, National Institute of Infectious Diseases, 1-23-1 Toyama, Shinjuku-ku, Tokyo 162-8640, Japan. Phone: 81 3 5285 1111. Fax: 81 3 5285 1189. E-mail: tokunaga@nih.go.jp.

minant of the fusion activity and infectivity enhancement and that glycine 36 of gp41, commonly seen in pL2 and the parental pLAI, is conserved in nearly all HIV-1 isolates except for pNL4-3 (and, surprisingly, T-20 escape mutants), which carry aspartic acid at this position (36D). By exploiting structural modeling of gp41, we were able to predict the cause of the fusogenic difference between L2/LAI and NL4-3 viruses. Together with the finding that escape mutants from the T-20 fusion inhibitor harbor the same 36D mutation (24, 27, 35, 40, 42), these results imply a molecular basis for the emergence of viruses resistant to this drug.

MATERIALS AND METHODS

Plasmid construction. To introduce a unique restriction enzyme site at the 3′ end of the envelope gene, a PCR-amplified BamHI-NotI fragment (nucleotide positions 8465 to 8786) and an amplified NotI-XhoI fragment (positions 8787 to 8887) from pNL4-3 (1) were ligated into pNL4-3 digested with BamHI and XhoI restriction enzymes (pNL-e-Not). To further introduce unique restriction enzyme sites into an *env* sequence, the SalI-NotI fragment (positions 5785 to 8786) of pNL-e-Not was subcloned into pBlueScript SK(+) (Stratagene) (pBS-NL-S/N). MroI and BlpI sites were introduced immediately upstream of the envelope signal peptide sequence (positions 6214 to 6219) and cleavage signal sequence (positions 7715 to 7721), respectively, on pBS-NL-S/N, and this construct was designated pBSNL-S/N-M/B. The SalI-NotI region of pBSNL-S/N-M/B was cloned back into pNL-e-Not to create pNL-envCT. An envelope gp41-coding sequence derived from pLAI was PCR amplified and inserted into pNL-envCT, to generate the proviral clone pNL-LAIgp41. An envelope gp120 sequence from pLAI was also PCR amplified and subcloned into MroI- and BlpI-digested pBSNL-S/N-M/B, and then the SalI-BlpI fragment was replaced with either pNL-LAIgp41 or pNL-envCT, to generate the proviral clone pNL-LAIgp160 or pNL-LAIgp120, respectively. In order to generate more recombinants of gp41, the NheI (positions 7250 to 7255)-XhoI (positions 8887 to 8892) fragment of pNL-envCT was inserted into a pGL3-Basic vector (Promega) and designated pGL3NL-N/X-Blp. Either the BlpI-HindIII (positions 7715 to 8136) or HindIII-BamHI (positions 8131 to 8470) fragment derived from pLAI was inserted into pGL3NL-N/X-Blp. The BlpI-NotI fragment of each plasmid carrying either BlpI-HindIII or HindIII-BamHI of pLAI was inserted back into pNL-envCT to create pNL-LAIgp41-1 and pNL-LAIgp41-2, respectively. To generate the proviral clone pNL-LAIgp41-3, a PCR-amplified BamHI-NotI fragment of pLAI was directly inserted into pNL-envCT. Chimeric proviral clones carrying pL2-derived sequence were also constructed by using the same strategies. These proviral clones were designated pNL-L2gp160, pNL-L2gp120, pNL-L2gp41, pNL-L2gp41-1, pNL-L2gp41-2, and pNL-L2gp41-3. To introduce the amino acid mutation 21Cys→Ala, 22Thr→Arg, 36Asp→Gly, 22Thr→Ala, or 91Leu→Phe, QuikChange mutagenesis (Stratagene) was performed by using pGL3NL-N/X-Blp as a template DNA. The resultant BlpI and NotI fragments were inserted into pNL-envCT, and the constructs were designated pNL-gp41-C21A, pNL-gp41-T22R, pNL-gp41-T22A, pNL-gp41-D36G, and pNL-gp41-L91F, respectively. Similarly, an amino acid change of 36Gly→Asp was introduced into pNL-1549 harboring a primary isolate (QH1549)-derived Env protein (37) to create pNL-1549-G36D. To quantify the infectivity, the PCR-amplified NotI-XhoI fragment of the luciferase (Luc) gene was inserted into NotI-XhoI region of pNL-envCT, pNL-gp41-D36G, pNL-1549, or pNL-1549-G36D and designated pNL-Luc-envCT, pNL-Luc-gp41-D36G, pNL-Luc-1549, or pNL-Luc-1549-G36D, respectively. Env expression plasmids pNLnΔBs (NL-Env expression plasmid) and pNLnΔBs-Nh (ΔEnv control plasmid) were previously described (38). pNLnΔBs-D36G was constructed by replacement of the NheI-BamHI region of pNL-gp41-D36G in the corresponding sites of pNLnΔBs. To generate pLTR-hLucP+, the 5′ long terminal repeat (LTR) sequence of pNL4-3 was PCR amplified and inserted into pGL3(R2.1)-Basic vector carrying the Rapid Response luciferase gene (Promega). To generate a Tat expression plasmid, pLTR-Tat, the *tat* sequence of pNL4-3 was PCR amplified and replaced with the humanized Luc gene from pLTR-hLucP+. To generate pNL-Δenv, an envelope-defective control vector, a frameshift mutation was introduced into the NdeI site within *env* gene of pNL4-3.

Cell maintenance and transfection. MOLT-4, M8166, CEMx174, H9, 293T, and MAGIC5A cells were maintained as described elsewhere (30, 32, 38). To prepare viral supernatants, 7×10^5 293T cells were transfected with 2 μg of each proviral expression plasmid by using FuGENE 6 (Roche). Sixteen hours later, cells were washed with phosphate-buffered saline (PBS), and then 2 ml of fresh complete medium was added. Twenty-four hours later, supernatants were filtered through 0.45-μm-pore-size filters. Levels of virion production were quantitated by HIV-1 p24 antigen capture enzyme-linked immunosorbent assay (ELISA) (Retro-Tek).

Syncytium formation assay. MOLT-4, M8166, CEMx174, or H9 cells (5×10^4) were incubated with 200 ng of p24 antigen of each virus at 37°C. After incubation for 48 h, the cells were fixed with 4% paraformaldehyde in PBS, and the formation of syncytia was observed under a light microscope.

Viral infectivity assay. MAGIC5A cells (5×10^5) were incubated with viral supernatants containing 10 ng of p24 antigen. Forty-eight hours after infection, cells were lysed in 100 μl of lysis buffer (Promega), and Luc activities were measured by MicroLumat LB 96V (Berthold).

Viral binding assay. One hundred nanograms of p24 of NL-Δenv (control), NL-envCT (wild type [WT]), or NL-gp41-D36G (D36G mutant) virus was added to 1.5×10^6 MAGIC5A cells at 4°C. After 3 h of incubation, cells were washed three times with PBS and then lysed in 100 μl of lysis buffer. The p24 antigen content of the lysates was measured by ELISA. The background obtained with control viruses was subtracted from sample values.

Cell-cell fusion assay. 293T cells as effector cells and MAGIC5A cells as target cells were transfected with pNLnΔBs (WT-env), pNLnΔBs-D36G (D36G-env), or pNLnΔBs-Nh (control env), plus pLTR-Tat, and with pLTR-hLucP+, respectively. After 48 h, both cell types were washed, trypsinized, and cocultured in a 12-well plate. After 5 h of incubation, cells were lysed in 200 μl of lysis buffer, and Luc activities were measured with a MicroLumat LB 96V. Transfection efficiency was normalized by cotransfection of 293T with phRL-CMV (Promega), which expresses a renilla luciferase.

Molecular modeling of the HIV-1 gp41 ectodomain trimer. To construct three-dimensional (3-D) structures of intact ectodomain trimers, we used the crystal structure of the simian immunodeficiency virus gp41 ectodomain trimer at a high resolution at 1.47 Å (Protein Data Bank code 1QBZ) (48) as a template for homology modeling. Although several other crystallographic structures of the HIV-1 gp41 ectodomain are available from the Protein Data Bank, those structures are either monomers or trimers lacking a majority of the N helix, C helix, and loop connecting the helices. 1QBZ has a sequence similarity of 52.5% to the target NL4-3 gp41 ectodomain, which is high enough to construct high-accuracy models with a root mean square distance (RMSD) of ~1 Å for the main chain between the predicted and actual structures (2). Monomer chains termed A, B, and C in the trimer structure 1QBZ lack 21, 9, and 3 amino acid residues, respectively. To minimize effects of the missing residues on the modeling, 1QBZ was modified by superimposing the chain C residues, which carry the fewest missing residues, on the chain A and chain B residues, and the modified 1QBZ structure was used as a template structure for modeling. 3-D models of HIV-1 gp41 ectodomain trimers of NL4-3 and the D36G mutant were constructed independently by the homology modeling technique using MOE-Align and MOE-Homology in the Molecular Operating Environment (MOE) (Chemical Computing Group Inc.). The 3-D structures were thermodynamically optimized by energy minimization using the MOE and a CHARMm22 force field. Physically unacceptable local structures of the optimized 3-D models were further refined on the basis of evaluation by Ramachandran plot and chi plot using programs packaged in MOE. We also tested distinct procedure for the modeling. In this case, we first made the NL4-3 gp41 model alone from the simian immunodeficiency virus template structure and then substituted the amino acid at position 36 from D to G, followed by energy minimization. This procedure generated a structure indistinguishable from the D36G structure obtained by the first procedure. Thus, we used structures made by the first procedure in the present study.

RESULTS

Ability of envelope gp120- and gp41-chimeric viruses to form syncytia. We first constructed a cassette vector, pNL-envCT, for envelope recombination. pLAI- and pL2-derived gp160 fragments were PCR amplified and cloned into pNL-envCT to generate pNL-LAIgp160 and pNL-L2gp160. The resultant chimeric viruses carrying the entire gp160 envelopes of pLAI and pL2 were analyzed in a syncytium formation assay. As expected, full-length Envs from pLAI and pL2 were fully able to support high-level fusion activity (Fig. 1), while NL4-3 Env did not reveal such a fusion activity under our experimental conditions. Since a significant number of reports

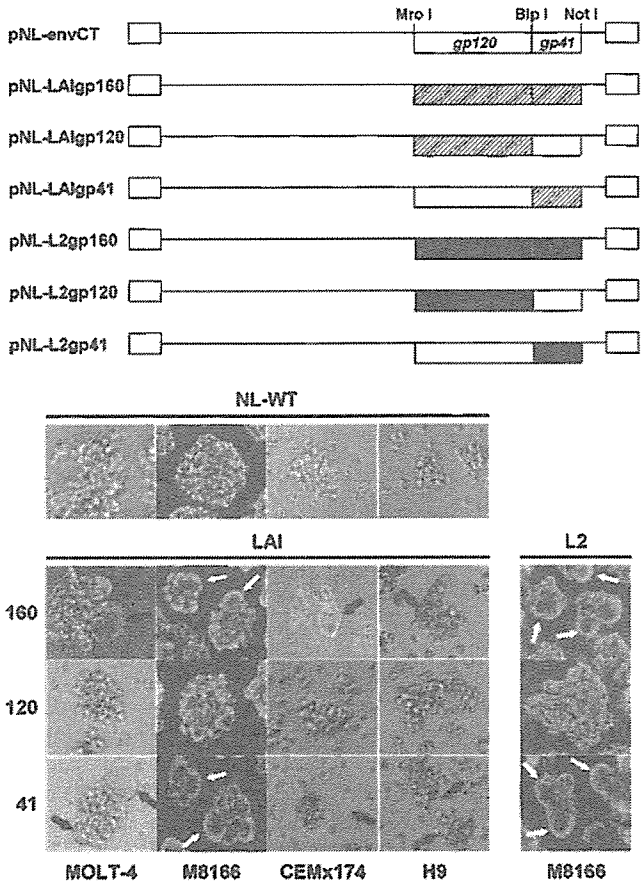

FIG. 1. Construction of gp120 and gp41 chimeric full-length proviral DNAs and their syncytium-forming activities. An HIV-1 envelope cassette vector, pNL-envCT (WT), harbors MroI, BlpI, and NotI restriction enzyme sites immediately upstream of the gp120, gp41, and *nef* genes of pNL4-3, respectively. The envelope gp160, gp120, and gp41 genes of pLAI and pL2 were replaced with the corresponding regions of pNL-envCT. MOLT-4, M8166, CEMx174, or H9 cells (5×10^4) were incubated with 200 ng of p24 antigen of each virus. After 48 h, cells were fixed and observed by microscopy. Arrows indicate the formation of syncytia.

regarding the role of gp41 envelope in fusogenic activity have been accumulated (4, 5, 12, 15, 19, 33), we attempted to assess whether pLAI- and pL2-derived gp41 could indeed determine the ability to induce high fusogenic activity. The gp120 or gp41 region derived from pLAI or pL2 was cloned in place of the equivalent *env* sequence present in pNL-envCT, and the abilities of these envelope-chimeric HIV-1 proviral clones to induce fusion activity were analyzed. As shown in Fig. 1, NL-LAIgp41 and NL-L2gp41 revealed high fusion activity similar to that observed in NL-LAIgp160 and NL-L2gp160, while NL-LAIgp120 and NL-L2gp120 did not show any syncytium formation. Therefore, we conclude that pLAI- and pL2-derived gp41 envelopes indeed determine the ability to induce more fusogenic activity than pNL4-3-derived Env.

Determination of a key amino acid in gp41 associated with the fusion activity. To further facilitate an accurate comparison of the abilities of the *env* genes derived from each of these isolates to support syncytium formation, we recombined three different regions in gp41 by utilizing conserved HindIII and BamHI restriction enzyme sites and newly introduced BlpI and NotI sites on gp41. The resultant viruses were analyzed in the syncytium-formation assay. As shown in Fig. 2A, NL-LAIgp41-1 and NL-L2gp41-1, carrying BlpI-HindIII fragments of pLAI and pL2, were able to reproduce the highly fusogenic activity observed in the LAIgp160, LAIgp41, L2gp160, and L2gp41 viruses. Thus, we found that the fusogenic activity of L2/LAI viruses was determined by an amino-terminal domain of gp41.

To identify the determinant of the syncytium-forming activity at the amino acid level, we performed site-directed mutagenesis. Since the amino-terminal domain of gp41 of pLAI or pL2 harbors three or four different amino acids, respectively (two amino acid differences are common in both clones), a total of five amino acid changes were introduced into pNL4-3: 21C→A (common in pLAI and pL2), 22T→R (pLAI type), 22T→A (pL2), 36D→G (common in pLAI and pL2), and 91L→F (pL2) of gp41; the constructs were designated pNL-gp41-C21A, -T22R, -T22A, -D36G, and -L91F, respectively. As shown in Fig. 2B, only the D36G mutation, which is common between L2 and LAI, led to syncytium formation. No significant difference in the Env gp120 and gp41 protein expression was observed among all viruses tested here (data not shown). Importantly, this activity was correlated with enhancement of viral infectivity (~5.5-fold [Fig. 2C]). We therefore conclude that the single amino acid substitution 36D→G is sufficient for the altered syncytium formation activity. This was surprising since we originally sought to identify the determinants of L2-specific fusion activity. Instead, we found that 36G of gp41 is well conserved among nearly all HIV-1 isolates according to the HIV-1 sequence database and that NL4-3 is rather exceptional in that gp41 harbors 36D, as reported in the T-20 studies (24, 35, 40, 42). The implications of this result are considered in Discussion.

Effect of the 36G→D mutation in a primary-isolate-derived Env. To further investigate whether these phenomena could be observed in a primary isolate, we utilized pNL-1549, encoding a primary-isolate-derived Env, in which amino acid position 36 of gp41 is glycine. We constructed the 36D version of this clone, termed pNL-1549-G36D. As shown in Fig. 3A, the mutant virus totally lost its syncytium-forming activity, while the WT virus displayed robust syncytium formation activity. Consistently, infectivity of the mutant virus showed an ~3.5-fold reduction (Fig. 3B). We therefore conclude that the effects of amino acid substitution at position 36 on syncytium formation and viral infectivity are reproduced in the primary isolate.

Effect of the D36G mutation on viral binding activity. Next, we attempted to clarify whether the effect of the D36G mutation on the syncytium formation might be regulated by viral binding activity due to an altered interaction between gp41 and gp120. Before testing this, we first quantitatively compared the difference in the fusion activity between WT NL and the D36G mutant Envs by performing a cell-cell fusion assay. In this assay, 293T cells as effector cells were transfected with Tat and Env expression plasmids, while CD4/coreceptor-expressing MAGIC5A cells as target cells were transfected with a plasmid carrying a synthetic version of rapidly responding Luc reporter gene which is driven by the HIV-1 LTR. After coculturing effector cells and target cells, fusion activity can be quantitated by measuring Tat-induced Luc activity. Transfection efficiency was normalized with renilla luciferase expression in the effec-